Predicting the Trajectory of Any COVID19 Epidemic From the Best Straight Line

Michael Levitt[1*], Andrea Scaiewicz[1], Francesco Zonta[2]

[1]Department of Structural Biology, Stanford School of Medicine, Stanford, CA 94305, USA
[2]Shanghai Institute for Advanced Immunochemical Studies, ShanghaiTech University, Shanghai, China

*Corresponding Author

ABSTRACT

A pipeline involving data acquisition, curation, carefully chosen graphs and mathematical models, allows analysis of COVID-19 outbreaks at 3,546 locations world-wide (all countries plus smaller administrative divisions with data available). Comparison of locations with over 50 deaths shows all outbreaks have a common feature: $H(t)$ defined as $\log_e(X(t)/X(t\text{-}1))$ decreases linearly on a log scale, where $X(t)$ is the total number of Cases or Deaths on day, t (we use $\ln$ for $\log_e$). The downward slopes vary by about a factor of three with time constants (1/slope) of between 1 and 3 weeks; this suggests it may be possible to predict when an outbreak will end. Is it possible to go beyond this and perform early prediction of the outcome in terms of the eventual plateau number of total confirmed cases or deaths?

We test this hypothesis by showing that the trajectory of cases or deaths in any outbreak can be converted into a straight line. Specifically $Y(t) \equiv -\ln(\ln(N / X(t))$, is a straight line for the correct plateau value N, which is determined by a new method, Best-Line Fitting (BLF). BLF involves a straight-line facilitation extrapolation needed for prediction; it is blindingly fast and amenable to optimization. We find that in some locations that entire trajectory can be predicted early, whereas others take longer to follow this simple functional form. Fortunately, BLF distinguishes predictions that are likely to be correct in that they show a stable plateau of total cases or death (N value). We apply BLF to locations that seem close to a stable predicted N value and then forecast the outcome at some locations that are still growing wildly. Our accompanying web-site will be updated frequently and provide all graphs and data described here.

INTRODUCTION

In December 2019 a coronavirus, known as SARS-CoV-2, was discovered in Wuhan China (Wang, 2020). The virus, perhaps from horseshoe bats (Zhou, 2020), spread between humans during January 2020, leading to the COVID-19 pandemic. Early prediction of the number of cases and deaths in an epidemic or pandemic is of vital importance as it helps policy makers make informed decisions on the best allocation of resources and containment of the pathogen. For this reason, many different groups have attempted to make reliable predictions of Sars-Cov-2 diffusion (Levitt 2020a, Wang 2020, Dimeglio 2020, Wu 2020, Pinotti 2020). These forecasts are based on a variety of mathematical and statistical models, which use different types of data (COVID-19 data, mobility data, demographic data) and take into account the impact of interventions, such as social distancing, proper hand hygiene and the use of masks. Such variables differ from country to country, and moreover, the criteria to detect COVID19 cases and consider COVID19 as the cause of deaths also vary sometimes even for states/provinces in the same country. These factors combine to complicate finding a universal method to fit and predict COVID-19 trajectories.

We began working on COVID-19 in the last week of January 2020 using data released by Sudalai Rajkumar (Rajkumar), Johns Hopkins Coronavirus Resource Center (JHCS) and Chinese internet (JOBTUBE). On January 28th, there were numbers of cases and deaths for 6 days starting on January 22nd. The daily death rate of COVID-19 (ratio of total deaths to total cases on a given day) was ten times higher inside Hubei, the province surrounding Wuhan, than everywhere else in China (non-Hubei). Concerned and encouraged by this data, we started an Excel spreadsheet to follow the daily progression of COVID-19. Each day, we made graphs of four simple measures. Three were obvious: the total number of cases; the total number of deaths, and their ratio, the death rate. The fourth was trivial but less obvious: the ratio of the total cases (or deaths) denoted as $X(t)$ for today divided by that of yesterday. This 'fractional change function' $f(t)$ measures exponential growth of $X(t)$ with $f(t) = X(t)/X(t-1)$.

If the total today is always 10% more than yesterday the value today will be 1.1 times the value yesterday with $f(t)=1.1$. In fact, on January 29th, the number of deaths today divided by that of yesterday was 1.3. Were such exponential growth of 30% a day to continue, everyone on earth would die within 90 days. Analyzing the data more completely over the next few days, we noticed on February 2nd that the fractional change for deaths in Hubei showed a steady decrease from 30% on January 29th to 18% four days later. If this linear decrease of fractional change in deaths continued then deaths in Hubei would stop on day 67, when the fractional change became equal 1 can $X(t)$ was the same as $X(t\text{-}1)$. We reported this finding widely (Levitt, 2020b), although in retrospect, it was naïve to expect the linear decrease to continue.

Nevertheless, our early interest in the fractional change function remained for two reasons. Firstly, because of the mathematical simplicity of $X(t)/X(t-1)$ as compared to more accepted measures like R_t (Wallinga 2007; Ferguson 2013). Secondly, because, by analyzing the data of a small number of early epidemics (before mid-March 2020), we realized that the factional change function appears to have the same shape for multiple locations: it converges to 1 as fast as a decaying exponential (Levitt, 2020c). Furthermore, because the fractional change function is a ratio, it is not affected by different systematic counts of cases/deaths due to different criteria: two countries that apply different criteria for deciding when a person is infected but have the same day to day growth will have the same fractional change function, provided that the counting method is kept consistent within the country.

Elaborating further from this initial intuition we found a minimal mathematical model that allows us to consistently describe the spreading of the virus in different countries. We also were able to reduce the very complicated task of fitting inconsistent data sets to the fitting of a straight line for which extrapolations and quality controls are trivial. This allowed us to completely automate data fitting, extrapolation and assessment of the quality of fitting, all done simultaneously and at blinding speed (less than an hour of CPU for all the outbreaks in the world).

METHODS

Data Processing:

Data is synced daily to two different sources for world data, US and Italy data. World data and US data including county and states levels is taken from (JHU), available from (Starschema). Italy data at provinces level is taken from (Ita-regioni). (We thank Levitt-group members Dr. João Rodrigues and Dr. Frederic Poitevin for integrating these data sources into a master file).

For some location the data contains inconsistencies, which we call 'data glitches' and these are corrected as we did in our earliest analysis of the epidemic in Hubei, China (Levitt, 2020d). We were well-aware that any alteration of the raw data must be justified and carefully recorded as we do here. Such correction turns out to be important as the curve-fitting of the raw data is insensitive to random counting errors, allowing us to use the raw data without any smoothing, but is sensitive to systematic errors like these. There were three type of 'data glitches': 'mis-glitches', 'rise-glitches' and 'drop-glitches'. (1) *mis-glitches* occur when the data on a given day is not updated. Specifically, whenever two consecutive *X(t)* values (at times *t-1* & t) are identical, we alter the value at *t* to be the average of the values at times *t-1* & *t+1*. (2) *rise-glitches* occur when new cases or deaths not previously reported are discovered and released on a particular day. This first occurred in China Hubei on February 13th, when 13,000 cases detected clinically were added to the total. These cases did not occur on the day reported but rather over the preceding days, so we corrected for by rescaling the number of confirmed cases on days prior to 13th February by a constant factor greater than 1 (Levitt 2020d). The same correction was applied on a small number of instances when additional deaths or confirmed cases were reported on a specific day as having been unreported on previous days. Again, we added the deaths or confirmed cases to the previous days a fixed fractional increment (the complete list of with both types of correction is provided in the Supplementary Material). (3) *drop-glitches* occur when the total numbers at a given location are decreased on a particular day. This can never happen normally as totals always increase and is due to the realization that numbers reported previously include misidentified cases or deaths. This glitch is less common than the other two. It is corrected in the same way as the *rise-glitch* except that the factor multiplying total values on all previous days is less than 1.

Mathematical background

We consider $X(t)$, the discrete temporal series of cases (or deaths) in a given country, region or province. In the most general scenario, we assume that $X(t)$ obeys the following ordinary differential equation (ODE):

$$\frac{dX(t)}{dt} = X'(t) = s(t)X(t) \qquad (1)$$

In the discretized form the first derivative of $X(t)$ is $X'(t) = X(t-1) - X(t)$, which is the number of new cases on day t. Equation (1) simply states that the number of new cases on a certain day is proportional to the number of cases on the previous day.

The coefficient of proportionality $s(t)$ is not constant. It changes with time so as to take into account the dynamics of virus spreading, which may be affected by social distancing or the structure of social network interactions.

We are interested in a solution of Equation 1 that reaches a plateau value of N for a large t (often called a growth function). A general form for many different kinds of growth functions can be written as follows (Koya 2013)

$$X(t) = N\left[1 - Be^{-k\left(\frac{t-\mu}{\delta}\right)^{\nu}}\right]^{m} \quad (2)$$

Equation 2 describes a rich family of curves which comprises Richards functions (Richards 1959), generalized logistic functions, Weibull functions (Frechet 1927) etc. While the overall shape of these curves depends on the various parameters, the asymptotic behavior has the same analytical form for all the curves in the family. It is this behavior that allows us to introduce an important simplification that reduces the fitting of Equation 2 to fitting a straight line. It is easy to show that the following relationship holds in the limit of large t:

$$Y(t) \equiv -\ln(\ln(N / X(t)) = -\ln(\ln(N) - \ln(X(t)) = t/U + \text{const} \quad (3)$$

Equation (3) is true asymptotically for every function in the Koya Goshu family, and exactly true for the Gompertz function, $G(t)$, (Gompertz 1825). This function has been also used by other groups to fit data of COVID-19 trajectories (Castorina 2020, Catala 2020) and is shown in **Fig 1** and **Fig. S1**):

$$G(t) = Ne^{-e^{-(t-T)/U}} \quad (4)$$

We also consider another function, which is the logarithm of the fractional change function $f(t)$ defined above:

$$H(t) \equiv \ln(f(t)) = \ln(X(t) / X(t-1)) \quad (5)$$

For a Gompertz distribution $H(t)$ is a decaying exponential function with the same time constant U, associated with $Y(t)$:

$$H(t) = e^{-\frac{t-T}{U}} + const - . \quad (6)$$

A similar relationship is valid asymptotically for other growing functions with the same time constant.so analysis of the behavior of $H(t)$, provides a second method to derive the time constant U.

Data fitting and validation

The simple linear relationship in Equation 3 provides a remarkable tool allowing us to fit the trajectory of virus spreading and predict the end points (N) in different locations. Given a single data series $X(t)$, the best estimate for $ln(N)$ is determined as the value that maximizes the correlation coefficient of $Y(t)$ and t (Figure 1). The calculation of the correlation coefficient is very fast and can be completely automated for a large number of data, and implicitly it also provides a measure of the validity of the assumptions that lead to Equation 4.

This calculation can be updated day by day, and eventually, the extrapolation for $ln(N)$ will converge to the correct number. As we will show in the results section, in many cases the end point can be predicted accurately at a very early stage.

The pseudo-code for data fitting is the following:

```
Read in csv date, Total Cases, Total Deaths for all the world
location
Correct errors, in the date
Main loop for each location
for line_end to End {
     for line_start 10 to line_end-10{
          step lnN from lnN1 to lnN2 by dlN{
               x=day; y = ln(N)-ln(X(t))
               CC = correlation_coef(x,y)
               Find maximum CC
          } if best CC > threshold
          Keep line Y coordinates and the lnN values
     }
}
```

For each line_end, collect the predicted N values and histogram them to find the most common value that is then taken as the prediction for that particular line-end value. We are well aware that this method can be improved in many ways some of which we are currently exploring.

Data Smoothing

All data is smoothed using the LOWESS method (locally weighted scatter-plot smoothing) developed by W. S. Cleveland at Bell Labs in 1988 (Cleveland 1988). We use the original FORTRAN code written in Ratfor (Ratfor 1976) (https://www.netlib.org/go/lowess) and converted to Mortran (Mortran 1975). The parameter F (the fraction of points used to compute each fitted value) is set to 0.05, 0.07, 0.1, 0.12 and 0.14 for SMO1 to SMO5, respectively. In addition, the smoothed output Y-axis values for SMO4 and SMO5 are smoothed a second time using F=0.1. Smoothing is only applied to the total counts of cases and deaths. Well-aware of the distortions that smoothing can cause, we made sure that the smoothing did not introduce false features at the start or end of the time series. We also made sure that the smoothing did not move the location of the peaks as shown in **Fig. S3.** We also test the root-mean-square value of the change in total values caused by the five different levels of smoothing. When we do this for locations with more than 60 deaths and for locations with more than 1000 cases we find that the % RMS error average values are between 0.4% and 1.2% for F ranging from 0.05 to 0.14.

One problem when using smoothed data to test prediction, is that smoothing uses future data points that would not have been available on the day the prediction would have been made. We allow for this in estimating when new cases and deaths peak by taking the effective peak date for completed situations as half way between the actual peak date found in the smoothed data and the date at which the level has dropped past the peak to half peak height. We also generally avoid using smoothed data.

RESULTS

What To Expect From Simple Mathematical Functions

The most important result of this study is that the Gompertz function can be transformed into a straight line provided one knows the final plateau value of total counts of either cases or deaths, denoted here as N. This is shown in **Fig. 1** and provides the basic method we use to fit the observed data. Namely, vary the value of N to make the transformed Gompertz function $Y(t)$ into a straight line and then derive parameters from the fit. Although this result is asymptotically true for a broad class of growth functions, we find that the simple three parameter Gompertz growth function fits the trajectory of actual COVID-19 outbreaks very well (Fig. 2). Specifically, the logarithm of the slope of ln$(X(t))$ (called $H(t)$) decreases linearly with time meaning that the exponential growth rate (the slope of ln$(X(t))$) is never constant so that growth is never exponential. This linear decrease of $H(t)$ is not true for all growth functions: specifically, the sigmoid function starts with pure exponential growth (**Fig. 2, c-d**). We find this linear decrease of ln$H(t)$ is in fact a universal property of all outbreaks (Fig. 3) justifying the broad use of the Gompertz function here.

Classification of World COVID-19 Outbreaks

Table 1 lists those countries (89 in all) or regions (Italy, US & Canada, 147 in all) with more than 50 deaths or 1000 cases. The outbreaks have been classified by our completeness code that is based on the peaking of the number of new daily cases or new daily deaths. (See **Table 1** for explanation for explanation of the completeness code).

Fitting With a Straight Line

Fig 4 (a) shows the function $Y(t)$ for deaths in the many different locations (countries or regions of countries) which have reached a plateau, and for which the prediction of the final N is stable. It is evident that for all these locations the data generally follows a linear relationship thereby justifying *a posteriori* our working hypothesis. This observation is confirmed by the fact that the correlation coefficient with time of $Y(t)$ is close to 1 for the vast majority of the locations we examined. We also note that the time constants U (i.e. the inverse slope of the lines or the time-constant of decay) are very similar to each other, indicating the existence of universal properties in virus diffusion that are largely independent of the country.

When considering confirmed cases (**Fig. 4**), we observe more diverse behavior in the time course of $Y(t)$. While for some countries the linear relationship still holds (**Fig 4 (b)**), in other countries we notice deviation from linearity (**Fig. 4 (c)**), which could indicate the existence of multiple outbreaks, or could reflect a change in the method of counting cases.

By fitting $Y(t)$ to a single straight line, we can average multiple outbreaks into a single major outbreak which will follow a Gompertz distribution, where the parameters U and T are the slope and the x-axis intercept at $Y(t)$=0, of $Y(t)$. This approach allows us to obtain a uniform description for every time series $X(t)$ of cases and deaths in different parts of the world, but with loss of details for locations that do not follow a simple linear relationship.

While *a posteriori* fits describe the raw data well, extrapolations of the final plateau before a given day are still subject to large fluctuations, due to the (double) exponential nature of Gompertz law. In other words, when $X(t)$ is small compared to N, the fitting line varies approximately like ln(ln(N));.even large variation of N barely affects the quality of the fit. Vice versa, when $X(t)$ approaches N, $Y(t)$ becomes more and more sensitive to the correctness of the predicted value of N (**Fig. S2**) The consensus predicted value of N converges to a plateau value with time, and then it is followed by real data with some delay. This allows us to discriminate between locations in which confirmed cases (or deaths) have reached or are near to reach the plateau, and locations for which it is still impossible to predict the plateau.

A closer Look at Specific Locations

While COVID-19 trajectories share many properties, each outbreak has its own features, which affect our ability to forecast the outcome in terms of the plateau value N for both cases and deaths. These features are best appreciated using two types of graphs, the Four-Panel graph and the Best Line Prediction graph described carefully in **Fig. 5**, which shows these two graphs for Germany a large but well-behaved outbreak. The top panel of **Fig. 5(a)** shows that for smoothed data there are single peaks of new cases and new deaths, with the new deaths peaking 11 days after the new cases. This is almost exactly what we observed for the smaller and much earlier outbreak in China, non-Hubei, where deaths were most likely to occur 10 days after a case was confirmed (**Levitt, 2020f**); this suggests that this interval may be connected to the natural progression of the disease in well-managed scenarios. The same delay between cases and deaths is also seen (as it should be) in the second panel. The third panel shows the characteristic curvature recognized since our 14-Mar-20 analysis (Levitt 2020b). Together with the forth panel, it also reveals a small initial outbreak that started on 24-Jan-20, was contained and then followed by a much larger outbreak that started two weeks later and became clearly seen after another two weeks. The Best Line Prediction (BLP) graphs for Germany show in **Fig. 5 (b)** that from 1-Apr-20, the plateau value of total cases would have been well-predicted. For deaths, **Fig. 5 (c)** shows the eventual plateau value could have been predicted accurately on 10-Apr-20. The blue dots on these two graphs show that the predicted plateau values vary wildly and a prediction can only be made because many straight-line fits give a similar consensus N value.

In **Fig. 6** we show four other locations which have reached a plateau and for which the extrapolation has not changed significantly in the last few weeks. Although none of these locations are as clean as Germany (**Fig. 5**), one see that early predictions are unstable but converge to more realistic figures with time. **Fig. 6(a)** shows New York City to be well-behaved in terms the smoothed peaks of new cases and new deaths although deaths and cases seem to occur at the same time. This suggests a situation less under control than either China, non-Hubei or Germany. Nevertheless, the BLP graph shows that the final plateau value of N for deaths in New York City could have been predicted correctly on 10-Apr-20. The decay of $H(t)$ shown in the bottom panel of the four-panel graph is very clean suggesting a single outbreak. **Fig. 6(b)** shows Sweden to have very badly formed peaks of new cases and new deaths and deaths seem to occur before cases, an impossibility likely due to decreased counting of cases as the epidemic proceeds. The BLP graph predicts a plateau value that is not constant although it does look as if total deaths will plateau at about 6,000. **Fig. 6(c)** shows Russia to also have a very extended peaks of new cases and deaths. The number of new cases peaked 7 weeks ago but new deaths remain high. Nevertheless, the BLP graph shows that the predicted plateau value of N for deaths is increasing more and more slowly and may well converge to a value of about 16,000, almost double the current number of deaths. **Fig. 6(c)** shows Mexico deaths to be increasing even more rapidly than Russia and at present it is impossible to predict the plateau.

In **Table 2**, we compare the predictive power on the Best Line Prediction (BLP) with that of the Peak Detection Method (PDM). Checking all the converged locations where the current value is expected to close to the expected plateau value of N shows that the BLP is significantly better than the PDM. Both methods seem to be able to make their predictions at about the same time (on average, the PDM predicts two days earlier than the BLP based on our assumed value for the peak confirmation date.

In **Table 3** we look at the most active locations to identify cases where prediction of outcome could have significant impact. For this we use two criteria: First, that the forecast be reliable in that the plateau is stable in terms of its slope, its percent standard deviation and at least seven days at this plateau value. Second, that the forecast plateau is a significant increase over the current level.

At the moment of writing this manuscript, many countries or regions are still in the fast growing phase, and it is still impossible to predict the outcome of the epidemic in them (see **Table 3**). For others we can make predictions as shown in **Fig. 7**. Panels (a) & (b) show clearly that the BLP graph for Peru predicts a clear plateau for cases (N=478,000), but the predicted plateau for deaths is still rising rapidly. The plateau value for cases is almost double the current level of 257,000 making this a very meaningful forecast. Panel (c) shows that for Brazil the BLP predicts a stable plateau of 98,000, another very meaningful forecast, again almost double the current level of 47,000. Panel (d) shows that cases in Belarus are predicted to plateau at 82,000, although there is a less clear leveling. Panel (e) shows a split prediction for cases in the United Arab Emirates where there are two plateaus, at 49,000 and about 60,000, respectively; such splitting is very rare. Panel (f) shows that deaths in Kuwait are perhaps going to plateau at 400. Panels (a) to (c) are important forecasts with a meaningful impact, whereas those in panel (d) to (f) show the diversity of behavior making automatic forecasting a challenging problem.

Open Availability of all Data

All graphs and tables are available online using apps written by Dr. Scaiewicz. The app at http://levitt1.herokuapp.com/ shows the classification for different countries and updated numbers and graphs. The app at http://levitt.herokuapp.com/ shows the predictions in the Best Line graphs.

Availability of the Computer Codes

We would like to make the computer codes we use available to all but these are currently written in a variety of languages that few would want to use. While Dr. Scaiewicz uses clean self-documenting Jupyter Python notebook code, Dr. Levitt still develops in a FORTRAN dialect call Mortran (Mortran 1975) that he has used since 1980. The Mortran preprocessor produces Fortran that is then converted to C-code using f2c. This code is at least a hundred-fold faster than Python code. His other favorite language is more modern, but involves the use of the now deprecated language Perl and Unix shell scripts.

Nevertheless, the methods proposed here are simple; they are easily and quickly implemented by a skilled programmer. Should there be interest, we would be happy to help others develop the code and test them against ours. We also realize that there is ample room for code optimization. Some of the things that we have considered are pre-calculating sums of terms to convert computation of the correlation coefficient from a sum over N terms to the difference of two sums. Another way to speed the code would be to use hierarchical step sizes in a binary search to find the value of ln$N$ that gives the best straight line.

Our study involving as it did a small group working in different time zones and under extreme time pressure revealed that scientific computation nowadays faces a Babel of computer languages. In some ways this is good as we generally re-coded things rather than struggle with the favorite language of others. Still, we worry about the future of science when so many different tools are used. In this work we used Python for data wrangling and some plotting, Perl and Unix shell tools for data manipulation, Mortran (effectively C++) for the main calculations, xmgrace and gnuplot for other plotting, Excel (and Openoffice) for playing with data. And this diversity is for a group of three!

DISCUSSION

Non-Exponential Growth

It is evident from our data analysis that the growth of a COVID19 epidemic does not follow an exponential growth law even in the very first days, but instead its growth is slowing down exponentially with time. While all growth functions decelerate exponentially when approaching the plateau, the Gompertz function is unique in that it is decelerating from the first day, and thus can fit the first part of the COVID-19 outbreak. Moreover, its relatively simple functional form, allowed us to produce an efficient computer code to fit data in all different locations in a consistent way.

As would be expected, we find several examples in which this simple law is not followed, especially when looking at confirmed cases (deaths appear to follow the Gompertz Function more consistently). For some of these countries (e.g. Iran) it is evident that a second outbreak occurred well separated in time from the first. In other countries, (e.g. South Korea) we observe a change in the dynamics of the virus spread, which could be related to the adopted containment strategy or a difference in the level of testing. Even though such unusual dynamics cannot be predicted from the beginning, our fitting method is able to identify abrupt changes and will identify the slowest characteristic time and will, therefore, be able to produce a prediction for the new plateau.

We believe that the analysis in our study shows conclusively that COVID-19 epidemics grow according to the Gompertz Function and not the Sigmoid Function (Fig. 2). The main difference between these functional forms is that the Sigmoid Function starts off growing exponentially (it has a constant exponential growth factor) and then slows down (blue line in Fig. 2(c)). The Gompertz Function is never exponential but rather has a growth rate that decreases exponentially from the very first confirmed case. This does not make sense as when there are very few cases, it should be easy for each infectious individual to find people to infect, which would lead to exponential growth at the early stages of the outbreak. The Gompertz Function normally applies to conditions when the growth is constrained by some global resource. For example, bacteria growing with a limited food supply or a fire in an enclosure where oxygen is limited.

What is limited for coronavirus? First clues came from the large number of invisible cases indicated by the early serological studies by our Stanford colleagues (Bendavid 2020). More recently, a paper in Science (Silverman 2020) showed that millions of people were infected in the USA before there were known cases. The existence of invisible cases of individuals who are mildly symptomatic and, therefore, not counted as confirmed cases may explain the non-exponential behavior of COVID-19: the known cases cannot easily find people to infect as the hidden invisible cases have already infected them. We realize that other factors may limit growth. For example, the structure of the human interaction network can lead to sub-exponential growth (Moreno 2002). Still, we believe that as SARS-CoV-2 is so infectious, it does not have a problem finding people to infect early on due to the local network structure.

Initial sub-exponential growth is not a unique feature of COVID-19, but has been observed in previous viral outbreaks and needs to be taken into account to produce accurate predictions (Chowell 2016). Our method provides a quick way to analyze early epidemic data and identify and also quantify sub-exponential growth in terms of the time constant U.

Clean and Curate Data Carefully

An essential step for our study has been to clean and curate the data made available from so many different countries. Had we not filled in missing value or spread large changes back in time, the sensitive methods we use would fail. Of course, we need to document every step we take so as not to manipulate data in some arbitrary way. In taking this approach we were aided by the fact that we started the project very early on when there were just 24 data points: six days of cases and deaths in two regions of China (Levitt 2020c).

Another consequence of being so intimately connected with the data is that we had to collect data manually until the various repositories became established. We are now quite certain that the quality of data is more or less the same from all sources. The question of data reliability is often raised and we believe that the data has to obey so many rules of self-consistency that cheating would be almost impossible. For example, in Fig. 2, we see that the raw data from China, non- Hubei. which was available in late January is essentially indistinguishable from the data released for New Zealand two months later.

Sanity Tests To Prove We Do Not Inadvertently Cheat

In a study like this involving a huge body of data, computer programs written quickly and the intense pressure to get results out while they can still be useful, one needs to be very self-critical at every stage looking for computer bugs that could explain any good results that one finds. Specifically, we are trying to test our forecasting method by going back in time and trying to predict something that was not known then but is know now. Such a process, often called 'postdiction' in contrast to 'prediction', is extremely dangerous. We guard against it by running calculations with data sets that have been specially prepared to eliminate all data after a certain previous date. This is tricky in that one cannot use smoothed data as smoothing looks into the future to smooth the present. In this work we made a series of data sets going back into the past and showed that the results from a past date would have been obtained with a data set that did not include data after that date.

Work in progress

We have been studying COVID for five months and worked on all aspects of the analysis. Some of the related projects that we are working on include:

(a) Predict the future time-course of the epidemic and not just the plateau value N. This will involve better understanding of the two other parameters of the best line fit, U & T.

(b) In what ways are the detailed trajectories from various locations different? What affects the trajectory in terms of N and U: population size, population age/health, physical size of location, social distancing or lockdown measures?

(c) What is the burnout saturation value of N? What is the population fatality ratio if the infection runs its course?

CONCLUSIONS

This manuscript is being submitted as a preprint, which is something that we have never done before. We do this for two reasons. One is to make our discoveries available to all at a stage where they will still be useful. Another is to solicit broad criticism and comments that are essential to the scientific process.

ACKNOWLEDGMENTS

This analysis started as a team effort based on our 14-Mar-20 analysis (Levitt 2020b); besides the current authors, it involved Patrick Tam (Hong Kong, see www.covibes.org), Frédéric Poitevin, João Rodrigues and Fatima Pardo-Avila (all at Stanford). We also had discussions and shared ideas with Eran Bendavid (Stanford), Cathrine Bergh (Royal Institute of Technology, Sweden) and Siri Camee van Keulen (Utrecht University, The Netherlands). We are most grateful to them. We offer special thanks to João Rodrigues, for his automatic daily data updates and invaluable advice on writing Python apps.

This work was supported by a US National Institutes of Health award R35GM122543 to M.L. and by a National Natural Science Foundation of China Grant No. 31770776 to F.Z. Michael Levitt is the Robert W. and Vivian K. Cahill Professor of Cancer Research.

REFERENCES

(Bendavid 2020) E. Bendavid, B. Mulaney, N. Sood, S. Shah, E. Ling, R. Bromley-Dulfano, C. Lai, Z. Weissberg, R. Saavedra-Walker, J. Tedrow, D. Tversky, A. Bogan, T. Kupiec, D. Eichner, R. Gupta, J. Ioannidis, J. Bhattacharya. COVID-19 Antibody seroprevalence in Santa Clara County, California. https://doi.org/10.1101/2020.04.14.20062463

(Castorina 2020) P. Castorina, A. Iorio, D. Lanteri. Data analysis on Coronavirus spreading by macroscopic growth laws. *International Journal of Modern Physics C*, 2050103. https://doi.org/10.1142/S012918312050103X

(Catala 2020) M. Catala, S. Alonso, E. A. Lacalle, D. Lopez, P. Cardona, C. Prats. Empiric model for short-time prediction of COVID-19 spreading. *PLOS Computational Biology*. May 19 2020, p.1-14, https://www.medrxiv.org/content/10.1101/2020.05.13.20101329v1

(Wang 2020) C. Wang, P. W. Horby, F.G Hayden, G. F. Gao. A novel coronavirus outbreak of global health concern. *The Lancet*, **395**, Issue 10223, 470–473.

(Chowell 2016) G. Chowell, L. Sattenspiel, S. Bansal, C. Viboud. Mathematical models to characterize early epidemic growth. A Review. *Phys Life Rev*. 2016 Sep; **18**: 66–97.

(Cleveland 1988) W. S. Cleveland & S. J. Devlin (1988). Locally weighted regression: an approach to regression analysis by local fitting. *Journal of the American Statistical Association*, **83**:403, 596-610. https://doi.org/10.1080/01621459.1988.10478639

(Dimeglio 2020) C. Dimeglio, J. Loubes, B. Deporte, M. Dubois, J. Latour, J. Mansuy, J. Izopet. The SARS-CoV-2 seroprevalence is the key factor for deconfinement in France. *J Infect*. 2020 Apr 29 https://doi.org/10.1016/j.jinf.2020.04.031

(Ferguson 2013) A. Cori, N. M. Ferguson, C. Fraser, S. Caucheme A New Framework and Software to Estimate Time-Varying Reproduction Numbers During Epidemics, *American Journal of Epidemiology*, **178**, 1 November 2013, Pages 1505–1512, https://doi.org/10.1093/aje/kwt133

(Frechet 1927) M. Fréchet. Sur la loi de probabilité de l'écart maximum. *Annales de la Société Polonaise de Mathematique*, Cracovie, **6**: 93–116.

(Gompertz 1825) B. Gompertz. On the nature of the function expressive of the law of human mortality, and on a new mode of determining the value of life contingencies. *Philosophical Transactions of the Royal Society of London*. **115**: 513–585.

(Koya 2013) P. R. Koya, A. T. Goshu. Generalized Mathematical Model for Biological Growths, *Open Journal of Modelling and Simulation*, **1** No. 4 (2013), Article ID: 38842.

Levitt 2020a) .9.Analysis_of_Coronavirus-2019_Data_Michael_Levitt https://www.dropbox.com/s/pn9k4c9fa4cuior/9.Analysis_of_Coronavirus-2019_Data_Michael_Levitt.pdf?dl=0 (First China analysis that used curve fitting).

(Levitt 2020b) 1.The_Corona_Chronologies. Part I - China. Part II. Rest_of_World_Michael_Levitt,Stanford_r.pdf https://www.dropbox.com/s/ovlsfr53horcmsn/1.The_Corona_Chronologies.%20Part%20I%20-%20China.%20Part%20II.%20Rest_of_World_Michael_Levitt%2CStanford_r.pdf?dl=0 (14-Mar-20 China and World analysis).

(Levitt 2020c) 2.Analysis_of_Coronavirus-2019_Data_Michael_Levitt2.pdf https://www.dropbox.com/s/46lw7pcrlhpuu94/2.Analysis_of_Coronavirus-2019_Data_Michael_Levitt2.pdf?dl=0 (First analysis on 2 Feb 2020).

(Levitt 2020d) 14.Analysis_of_Coronavirus-2019_Data_Michael_Levitt https://www.dropbox.com/s/rja6r86da8ul0a6/14.Analysis_of_Coronavirus-2019_Data_Michael_Levitt.pdf?dl=0 (China analysis that corrected for 13 Feb. data)

(Levitt 2020e) 2. All_Michael_Levitt_22_Reports_on COVID-19_2-Feb-to-3-Mar.pdf https://www.dropbox.com/s/fp90jfszmyxut2g/2.%20All_Michael_Levitt_22_Reports_on%20COVID-19_2-Feb-to-3-Mar.pdf?dl=0 (Combine all 22 Analyses for China 2-Feb. to 3-Mar).

(Levitt 2020f) 28.Analysis_of_Coronavirus-2019_Data_Michael_Levitt.pdf https://www.dropbox.com/s/3oy8plmtgcupvjh/28.Analysis_of_Coronavirus-2019_Data_Michael_Levitt.pdf?dl=0 (Levitt Analysis of 10 day delay between Case and Death).

(Moreno 2002) Y. Moreno, R. Pastor-Satorras, A. Vespignani. Epidemic outbreaks in complex heterogeneous networks. *The European Physical Journal B-Condensed Matter and Complex Systems,* **26**, 4, 521-529.

(Mortran 1975) User Guide to Mortran3. http://rcwww.kek.jp/research/egs/epub/manuals/append4.html

(Pinotti 2020) F. Pinotti, L. Di Domenico, E. Ortega, M. Mancastroppa, G. Pullano, E. Valdano, P. Boëlle, C. Poletto, V. Colizza. Lessons learnt from 288 COVID-19 international cases: importations over time, effect of interventions, under-detection of imported cases. https://www.medrxiv.org/content/10.1101/2020.02.24.20027326v1

(Ratfor 1976) B. W. Kernighan and P. L. Plauger. Software Tools. Addison-Wesley Longman Publishing Co., Inc. Boston, MA,1976.

(Richards 1959) F. J. Richards. A flexible growth function for empirical use. *Journal of Experimental Botany*. **10**, 290-300. http://dx.doi.org/10.1093/jxb/10.2.290

(Silverman 2020) J. D. Silverman, N. Hupert, A. D. Washburne. Using influenza surveillance networks to estimate state-specific prevalence of SARS-CoV-2 in the United States. *Science Translational Medicine* 22 Jun 2020: http://dx.doi.org/10.1126/scitranslmed.abc1126

(Wallinga 2007) J. Wallinga and M. Lipsitch How generation intervals shape the relationship between growth rates and reproductive numbers, *Proc. R. Soc. B,* **274**, 599–604. http://dx.doi.org/doi:10.1098/rspb.2006.3754

(Wang 2020) H. Wang, Z. Wang, Y. Dong, R. Chang, C. Xu, X. Yu, S. Zhang, L. Tsamlag, M. Shang, J. Huang, Y. Wang, G. Xu, T. Shen, X. Zhang, Y. Cai. Phase-adjusted estimation of the number of Coronavirus Disease 2019 cases in Wuhan, China. *Cell Discov* **6**, 10 (2020). https://doi.org/10.1038/s41421-020-0148-0

(Wu 2020) Wu J.T., Leung K. Nowcasting and forecasting the potential domestic and international spread of the 2019-nCov outbreak originating in Wuhan, China: a modelling study. The Lancet. 2020; 395(3).

(Zhou 2020) P. Zhou, X. Yang, X. Wang, B. Hu, L. Zhang, W. Zhang, H. Si, Y. Zhu, B. Li, C. Huang, H. Chen, J. Chen, Y. Luo, H. Guo, R. Jiang, M. Liu, Y. Chen, X. Shen, X. Wang, X. Zheng, K. Zhao, Q. Chen, F. Deng, L. Liu, B. Yan, F. Zhan, Y. Wang, G. Xiao, Z. Shi. A pneumonia outbreak associated with a new coronavirus of probable bat origin. *Nature* **579**, 270–273 (2020). https://doi-org.stanford.idm.oclc.org/10.1038/s41586-020-2012-7

ONLINE RESOURCES USED OR CITED IN THE TEXT

(Rajkumar) https://www.kaggle.com/allen-institute-for-ai/CORD-19-research-challenge

(JHCS) https://gisanddata.maps.arcgis.com/apps/opsdashboard/index.html#/bda7594740fd40299423467b48e9ecf6

(JOBTUBE) https://jobtube.cn/wv/?from=groupmessage&isappinstalled=0

(JHU) https://s3-us-west-1.amazonaws.com/starschema.covid/JHU_COVID-19.csv

(Starschema) https://starschema.com/covid-19-data-set

(Ita-regioni) https://raw.githubusercontent.com/pcm-dpc/COVID-19/master/dati-regioni/dpc-covid19-ita-regioni.csv

(Levitt-Twitter) https://twitter.com/MLevitt_NP2013/status/1256511516863586304?s=20

LEGENDS FOR MAIN TABLE & FIGURES

Table 1: Showing the classification scheme we use for all worldwide outbreaks. The Classification Code consist of four symbols, two for Cases and two for Deaths that are initially set to '='. Position 1 is 'c' if New Cases per Day have reached a maximum and are dropping; position 2 is set to 'C" if New cases per Day have dropped to below half the maximum values; positions 3 & 4 are set to 'd' and 'D' when new deaths per day have reached a maximum or have dropped to half their maximum value. The determination of peaking is made using heavily smoothed data (SMO5) (see text).

Table 2: Comparing Best Line Prediction (BLP) and Peak Detection Method (PDM) for Prediction of Plateau N Value. The plateau N value predicted by the Best Line method is significantly more accurate than that predicted by the Peak Detection method. This can be measured by the Percent Error of the Prediction defined as 100*(Predicted_Plateau_Value - Value_Now)/(Value_Now). For the BLP method this number averages 11% for cases prediction and 9.5% for deaths prediction, whereas the corresponding values for the PDM are more than double at 25.3% and 23.7%, respectively. Another way to measure the advantage of BLP over PDM is to count for different locations how often BLP does better than PDM. Here BLP is better than PDM in 74% of the locations for cases and in 73% of the locations for deaths.

Table 3. Forecasts of Plateau N Ordered by Size and Certainty (green shading more certain but may involve small increases to plateau so less important). The locations here are not converged (their classification code is not 'cCdD'). Rather than look at the individual Best Line graphs manually, we do line fitting to the predicted plateau N working back from today. Key parameters are the slope of the line through the plateau values, which should **be** small, the Percentage Standard Deviation of the Plateau value (%SD) and the number of days with a plateau prediction within 20% of the predicted value.

Figure 1. (a) Basic properties of the Gompertz functions and its logarithms. The Gompertz function is an exponential of an exponential written as $G(t) = Ne^{-e^{-(t-T)/U}}$ or $G(t) = N\exp(-\exp(-(t-T)/U))$, and defined by three parameters N, T & U, each with clear physical meaning. Parameter N is the

asymptotic number, the maximum plateau value that $G(t)$ reaches after a long time, t. Parameter T, is the point of inflection, which is the time in days at which the second-derivative of $G(t)$ is zero and its first derivative is a maximum. It is a natural mid-point of the function where the value *of* $G(T)=N/e=0.37N$. The Parameter U, is the most important as it changes the shape of the curve; it is a time-constant measured in days.

Given the double exponential nature of $G(t)$, one might expect to use a double logarithm to simplify it. The function *G(t)* itself has the expected S-shape of saturating growth function. Taking the logarithm once gives $\ln(G(t)) = \ln(N) - \exp(-(t-T)/U)$, where ln is the natural logarithm or log_e ; it is shown in dashed line increasing very rapidly at first but curving steadily to become horizontal at saturation. Rearranging as $\ln(N) - \ln(G(t)) = \exp(-(t-T)/U)$and taking the logarithm a second time gives $Y(t) = -\ln[\ln(N) - \ln(G(t))] = -\ln[\ln(N/G(t))] = (t-T)/U$. This function is shown in the dotted line to be a simple straight line. This is hugely significant as extrapolation of a straight-line is trivial: just keep going straight. As we show in the text, the function $Y(t)$ is always a straight line for the Gompertz function. More generally, $Y(t)$, tends to a straight line for a very general class of saturating functions

(b) Illustrating how the linearity of the $Y(t)=-ln(ln(N/G(t))$ depends on the value of N. The linearity shown in (a) has an apparent weakness, namely the line is only straight when the value of N is the correct saturation value and this value will be unknown until the epidemic is over. This weakness is in fact a strength. One can try different values of N and find the one that gives a straight line. In fact, “straighten the line” is much more relevant than the saying “flatten the curve” popularly applied to COVID19.

Figure 2. Showing that the data from two outbreaks far apart in both space and time are almost indistinguishable. The raw data shows as colored circled of two well-controlled outbreaks in China, non-Hubei (all China except for Hubei Province) shown panels (a) & (c) and in New Zealand panels (b) & (d) are essentially identical. The fits for the data (solid lines) as also very similar except for the maximum plateau value of confirmed cases N=13,219 & 1,500, respectively) and the mid-point date in number of days from 23 January 2020, T=32.13 & 90.50. The U parameter is also very similar at U=5.87 & 5.88 days, respectively. Use of the Sigmoid Function in panels (c) & (d) give a fit that is less good that that obtained with the Gompertz Function in panels (a) & (b). This is shown by higher fit residuals (10.158 vs. 7.989 and 0.037 vs 0.035). More importantly, when compared to the

Gompertz function, the Sigmoid function is less able to capture the behavior at the start of the outbreak. Following our four-panel graphs, we plot the Total Number of Cases (black line for $X(t)$, on left-hand y-axis, which is a log-scale), the number of New Cases (red line for $X(t)-X(t-1)$, right hand y-axis, which is a linear scale), and Gradient of log Total Cases (blue line for $H(t) = ln(X(t)) - ln(X(t-1)) = ln(X(t)/X(t-1))$ on the left-hand y-axis, log scale). Note that for both the real data and the Gompertz function, ln[ln$[(X(t)/X(t-1))$]] is a linear function of time, t.

Figure 3. Showing the trajectory of $\ln[H(t)]$ or $\ln[\ln[X(t)/X(t-1)]]$ for all selected locations with more than 50 deaths. From **Fig. 2**, $\ln[H(t)]$ is expected to decrease linearly for the Gompertz function. As $H(t)=\ln[X(t)] - \ln[X(t-1)]$ is the difference of two numbers, it is subject to a high level of noise. For this reason, we smooth the $X(t)$ using SMO5 LOWESS smoothing. Panel (a) shows the trajectories of $\ln[H(t)]$ for cases. Panel (b) shows $\ln[H(t)]$ for deaths. As there are often relatively low numbers of deaths, the trajectories for deaths are still noisy even after smoothing (NB. The noise in some highlighted locations is unexpectedly high and warrants further investigation).

Figure 4. Showing the trajectory of $Y(t))$ or $-ln(ln(N/X(t)) = -ln(ln(N)-ln(X(t)))$ for all selected locations with more than 50 deaths. From **Fig. 1**, $Y(t))$ is expected to decrease linearly for the Gompertz function and, for more general growth functions in the limit of large t (see **Methods**). In panel (a) we show the raw data for $Y(t)$ for deaths in a selection of more than 130 locations (thin gray lines), and emphasize 5 representative ones with a thicker line. For all such selected locations, $Y(t)$ is well approximated by straight lines with a very similar slope. Panels (b) shows $Y(t)$ for confirmed cases in 119 locations. In panel B we emphasize locations for which the function $Y(t)$ is again well approximated by a straight line, while in Panel (c) we show some locations for which this is not true anymore. This is expected if multiple outbreak of comparable intensity happens in a country, or if there is change in the dynamics of infections or the way cases are counted.

Figure 5. Showing for Germany the Four-Panel graph (left) and Best Line Prediction (BLP) graphs right. In the Four-Panel graph, which has been carefully refined since Feb. 2020 to show the most relevant data in an epidemic, the top panel is New Cases per Day (red, left y-axis) and New Deaths

per Day (black, right y-axis) both normalized to the same height. The second panel is Total Cases and Deaths shown in their respective color and y-axis and also normalized. The third panel is these same totals plotted on a $\log_{10}$ scale (no need for normalization). The fourth panel is ln[($X(t)/X(t\text{-}1)$ plotted on a $\log_{10}$ scale (log of the fractional change used in our first analysis, Levitt 2020c). Here we consistently use $\log_e$ or $\ln$ for calculations as growth functions are defined in terms of the exponential, e; we use $\log_{10}$ to define logarithm y-axes as powers of ten are more familiar to us humans than are powers of e.

In the BLP graph, Dates are plotted along the x-axis and Total Number of either Cases or Death along the y-axis. The actual trajectory of total data counts is plotted as heavy black circles and increases monotonically with time. The horizontal red dashed line marks the maximum total count number on the latest day included (date specified in the title). The blue dots are the candidate predicted N plateau values (the predicted final completion total count) shown at the Date value where they were made. Specifically, only data up to including this date can be used to find the $\ln(N)$ value that gives the best line. The brown squares enclose the actual predicted N value that is found by most of the predictions at that date (most overlapping blue dots are in the boxes).

Figure 6. Showing four locations, which behave differently because they are at different stages of their outbreak. (a) Deaths in New York City, which was the hardest hit location with more deaths per population than anywhere else. The smoothed data in the lower part of the Four-Panel graph shows clean peaks for Cases and Deaths and a linear descent $H(t)$ on the log scale. The Best Line Prediction in the upper part shows that the plateau number of deaths was indicated as early as 4-Apr-20 and confirmed a week later. (b) Deaths in Sweden, which adopted very limited social distancing and no lockdown. The smoothed curve of new cases and new deaths remains elevated for much longer than in NYC although there is a very similar linear descent $H(t)$ on the log scale. The BLP seems to edge up but a good prediction of the current plateau could have been made on 22-Apr-20. This is 10 days earlier than a prediction of Sweden peaking we made on Twitter on 2-May-20 (Levitt-Twitter) showing the power of the BLP method that we did not have back then. (c) Confirmed Cases Russia are growing rapidly, although the number of new cases per day peaked on 8-May-20 they remain stable at a high level. The BLP method tentatively predicts a plateau N value of about 700,000 cases in Russia. (d) Deaths in Mexico are still far from any clear plateau value..

Figure. 7: Showing the BLP graphs for active locations with prediction approaching convergence of N (Peru, Brazil, Belarus, UAE, Kuwait)). These locations have been selected from **Table 3** because the predicted plateau is significantly higher than the current level (red dashed horizontal line). As this involves locations with large numbers of expected additional cases and deaths. Forecasting the outcome could be of major value to the countries involved. The locations also show a range of different behaviors.

Comment [M1]: TO DO

LEGENDS FOR SUPPLEMENTARY FIGURES

Figure S1. Showing how the U parameter has a major effect on the shape of the Gompertz Function, affecting as it does the trajectory of the Total Count ($X(t)$, in black), the new counts by day (($X(t)$-($X(t-1)$), in red) and the gradient of the ln(Total Counts), which is ln[$X(t)$]-ln[$X(t-1)$] or ln[ln[$X(t)/X(t-1)$]] (in blue). The solid lines show trajectories for the Total Counts, New Counts, and Gradient ($H(t)$) for a U parameter of 7 days, the shortest decay time seen for real cases (Table 2). The dotted lines show the same data for U= 4 days and the dashed line shows the same data for U=21 days . The trajectory of ln[$H(t)$], the gradient of ln[$X(t)$], is a simple straight line with slope of $1/U$

Figure S2. (a) Showing how straight line fits have strong predictive power. The lines in green are fitted to data that was available 50 days ago. The line in magenta is fitted to current data and is a straight-line continuation of the best line 50 days ago. The Correlation Coefficient (*CC*), which is used to measure the straightness of the line as a function of ln(N), is sensitive to departure from linearity. (a) Shows that as ln(N) varies the *CC* value reaches its maximum smoothly. (b) Distribution of correlation coefficients value as the guessed value of ln(N) is changed.

Fig S3. Showing our Four-Panel graphs with different levels of smoothing of the data using the LOWESS method (see text). The strength of the smoothing increasing progressively for SMO1 through SMO5 and one sees that while local ripples are eliminated there is no shift of the peak position. Such shift do occur with simpler smoothing schemes such a running averages.

Supplementary Methods

Proof that any growth function has a $Y(t)$ function that tend to be linear for large t.

$$\ln\left(\frac{X(t)}{N}\right) = m \ln\left[1 - Be^{-k\left(\frac{t-\mu}{\delta}\right)^{\nu}}\right]$$

$$\lim_{t\to\infty} Be^{-k\left(\frac{t-\mu}{\delta}\right)^{\nu}} = 0$$

$$\lim_{Z\to 0} \ln\ (1 - Z) = -Z$$

$$\ln\left(\frac{X(t)}{N}\right) = -Bme^{-k\left(\frac{t-\mu}{\delta}\right)^{\nu}}$$

$$-\ln\ln\left(\frac{N}{X(t)}\right) = Bm\nu k\left(\frac{t-\mu}{\delta}\right) = t / U + const$$

Fig. 1: **Showing the Gompertz Function $Y(t)$ Straightened to Line Y(y) to Predict Plateau N.**

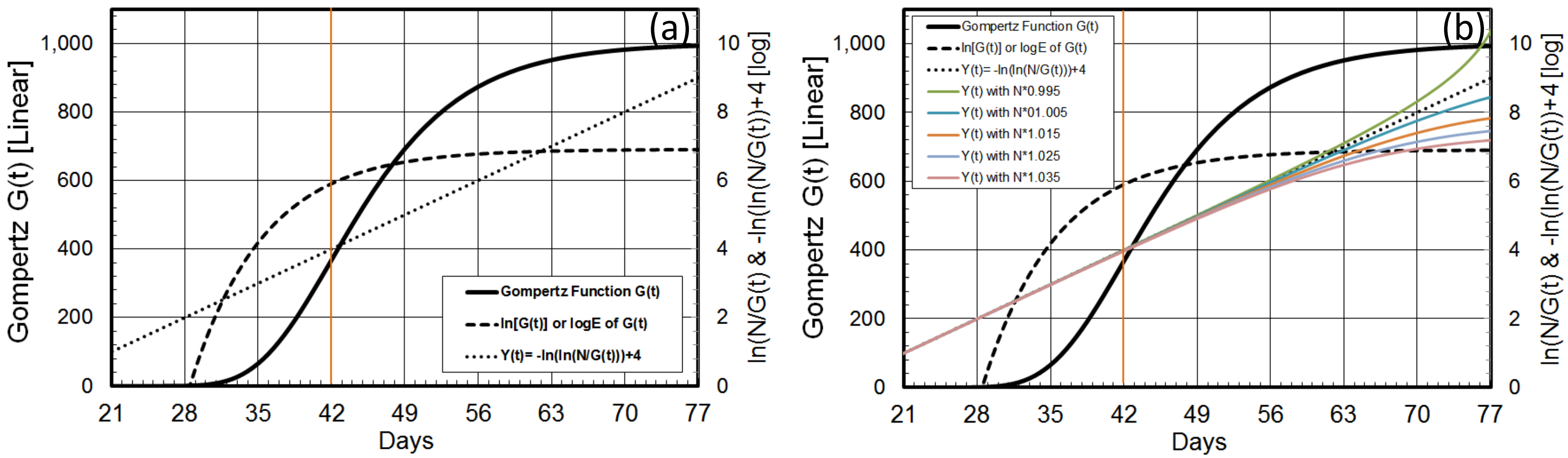

Fig. 2: Showing How Early Raw Data Analysis Shows Non-Exponential Growth.

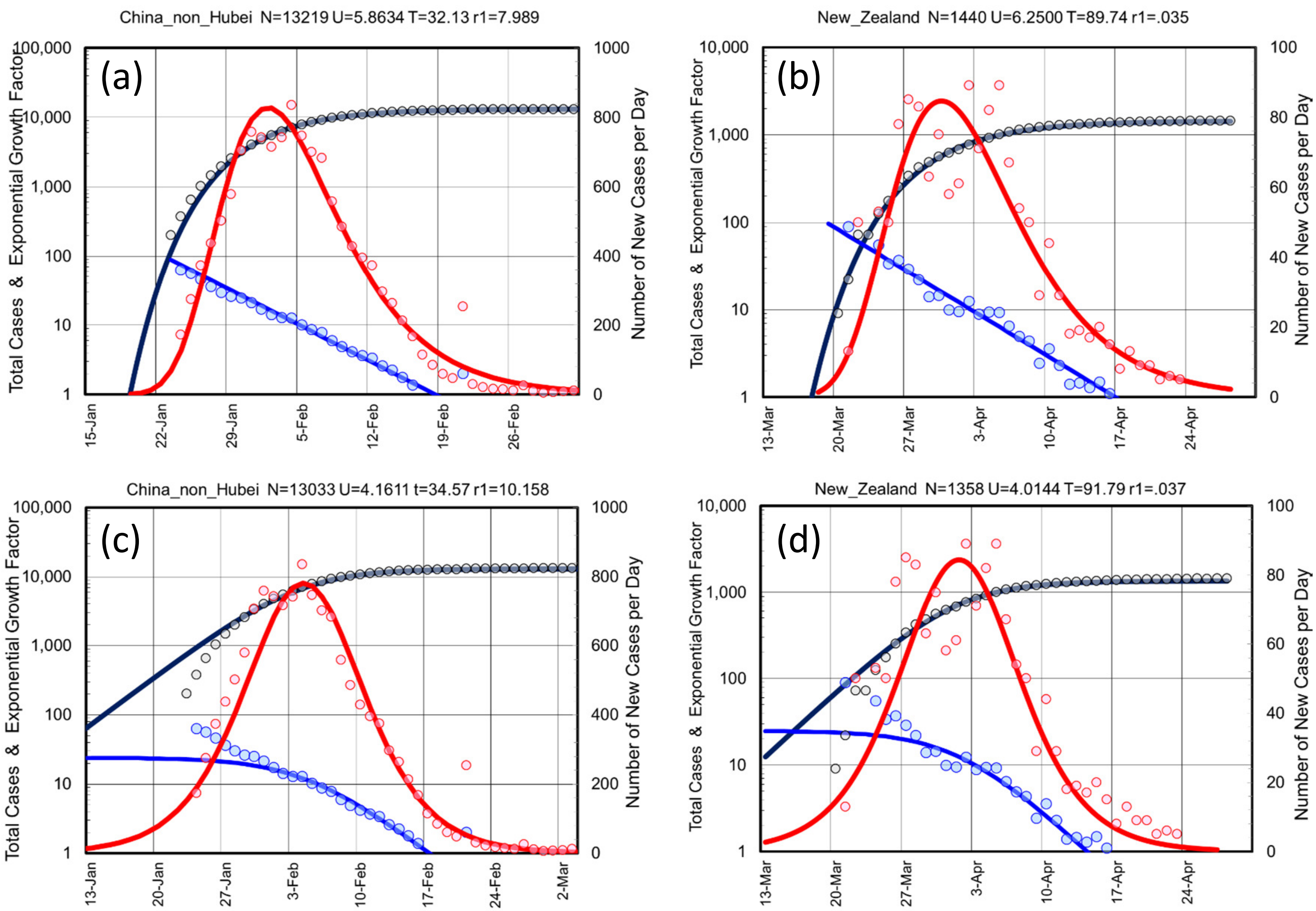

Fig. 3: Value *ln[H(t)]=ln[ln[X(t)/X(t-1)]]* Deceases Linearly as Expected for Gompertz Function. (data is smoothed with SMO5 as difference of small numbers)

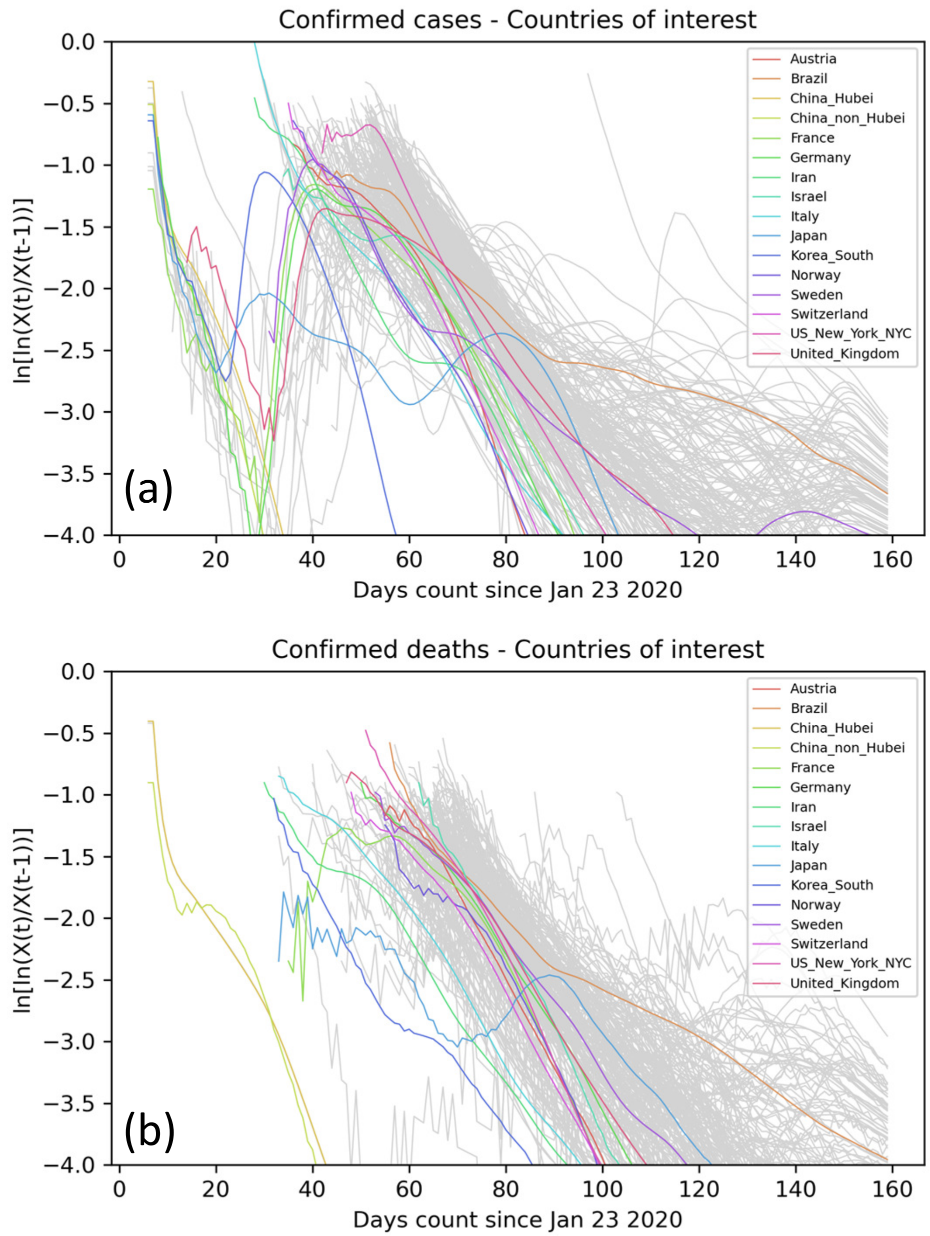

Fig. 4: Function *Y(t)=ln[ln[N/X(t)]]* Give Straight Lines for Raw Unsmoothed Data.

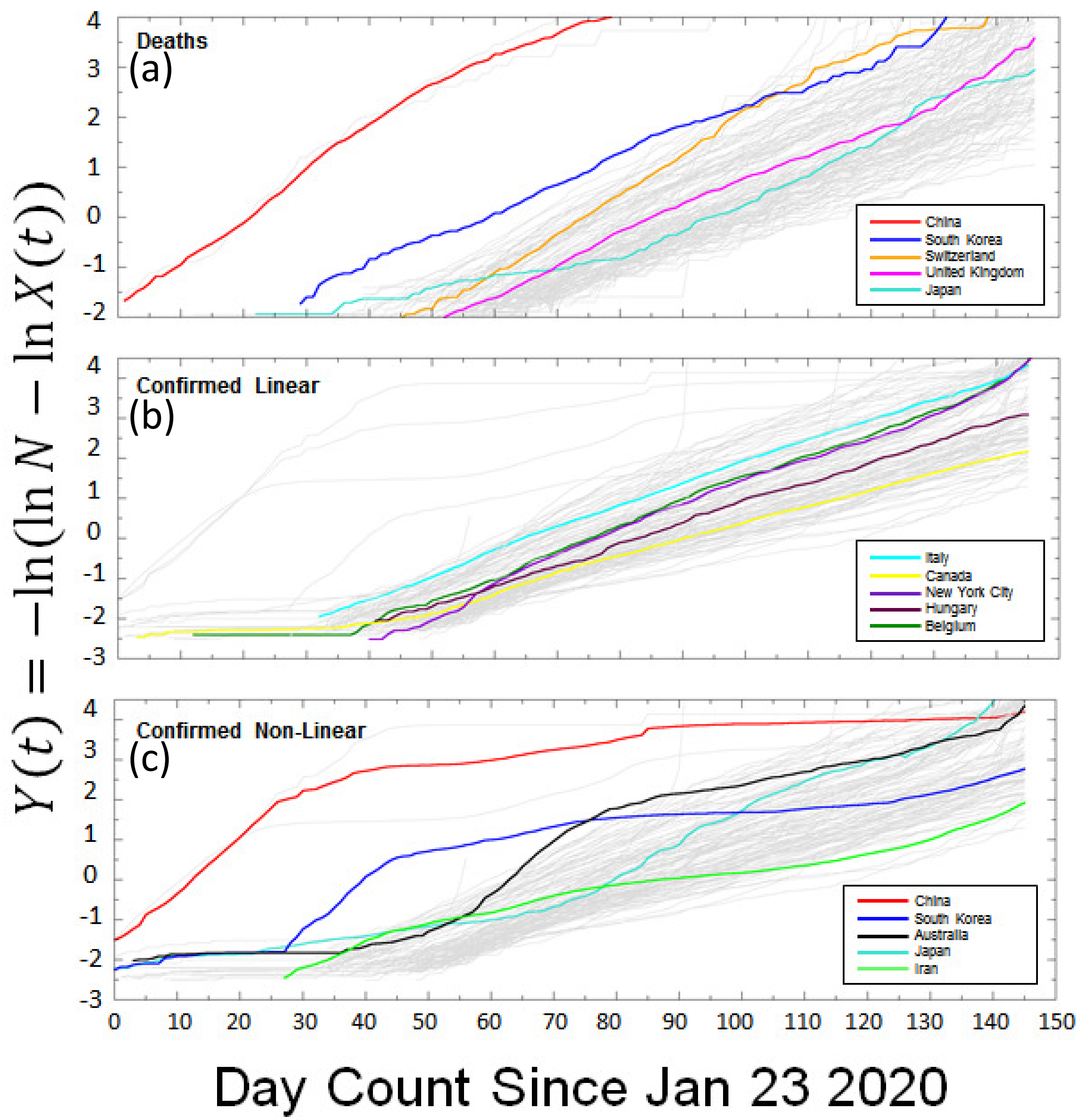

Fig 5: Showing Best Line and Smooth Peak Graphs for Germany.

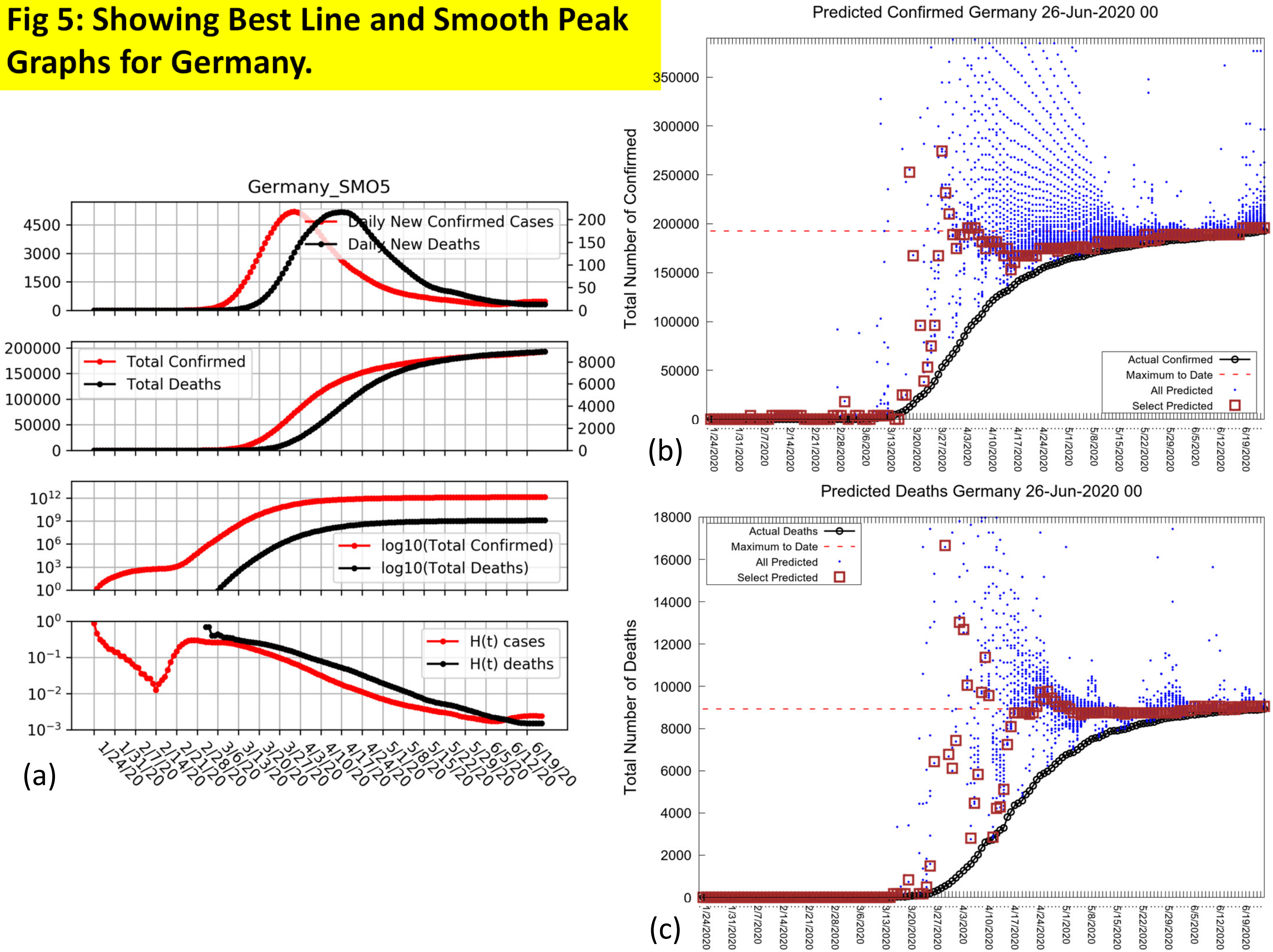

Fig 6: Plots showing Best Line and Smooth Peak Graphs for Selected Locations.

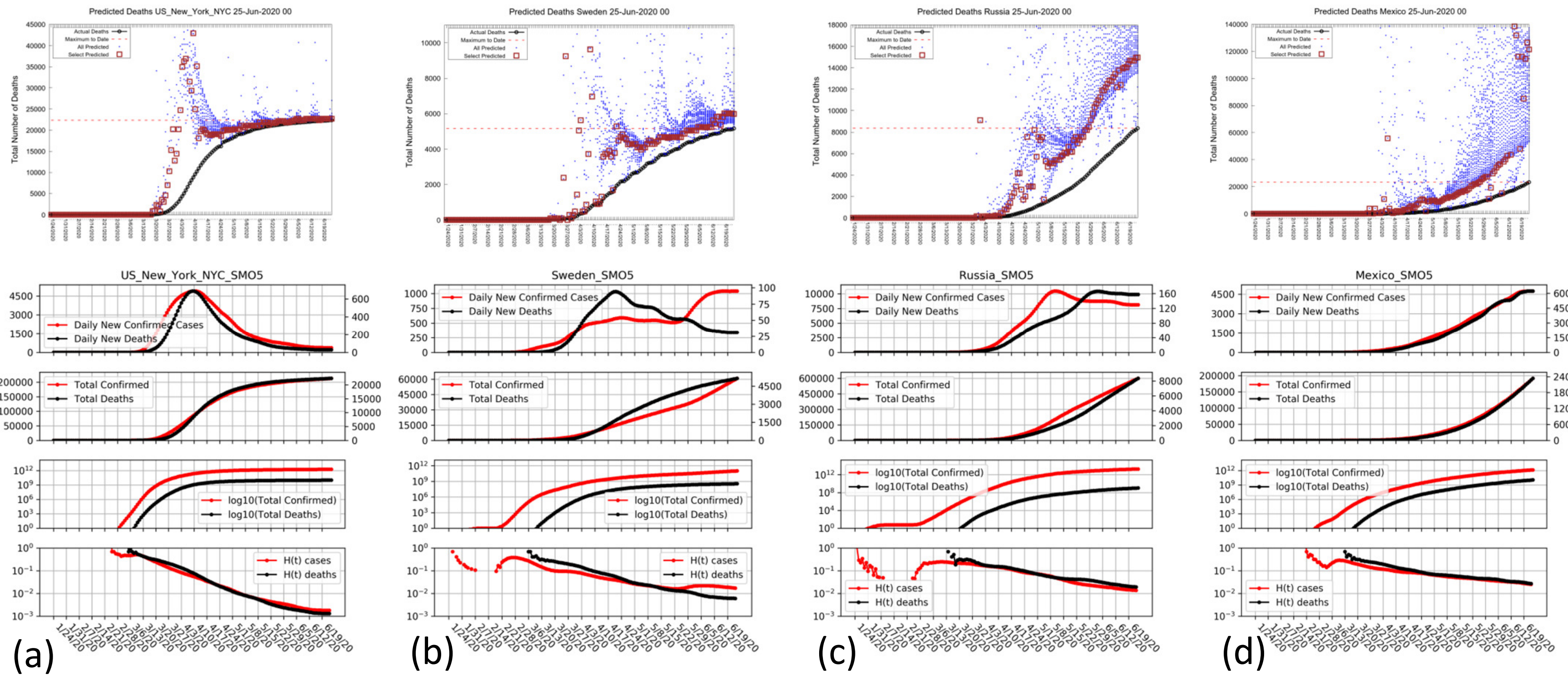

Fig. 7: Best Line Predictions for Six Active Locations Ready for Forecast.

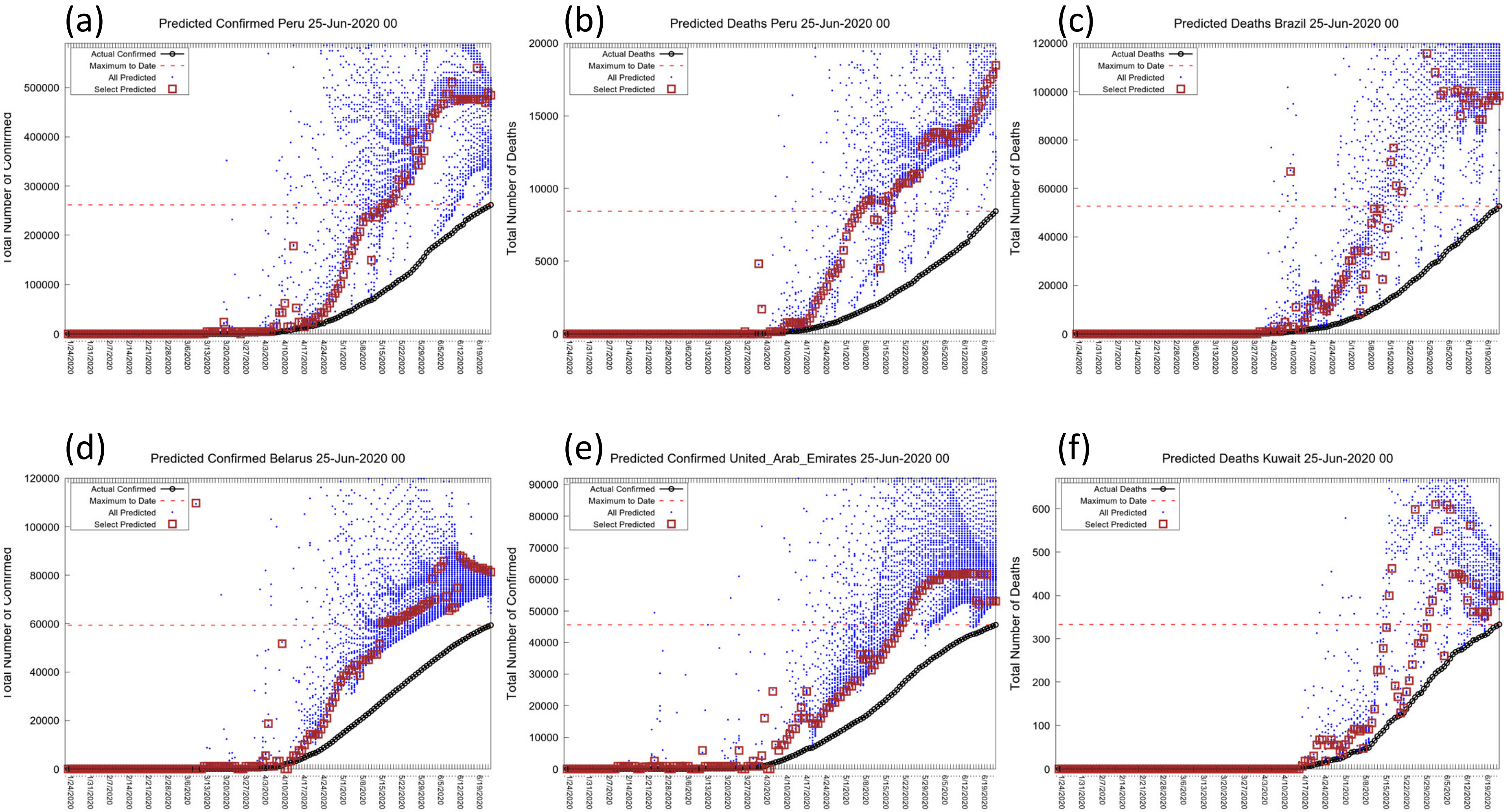

Fig. S1 Showing affect of the parameter U (in days) on the Gompertz Function.

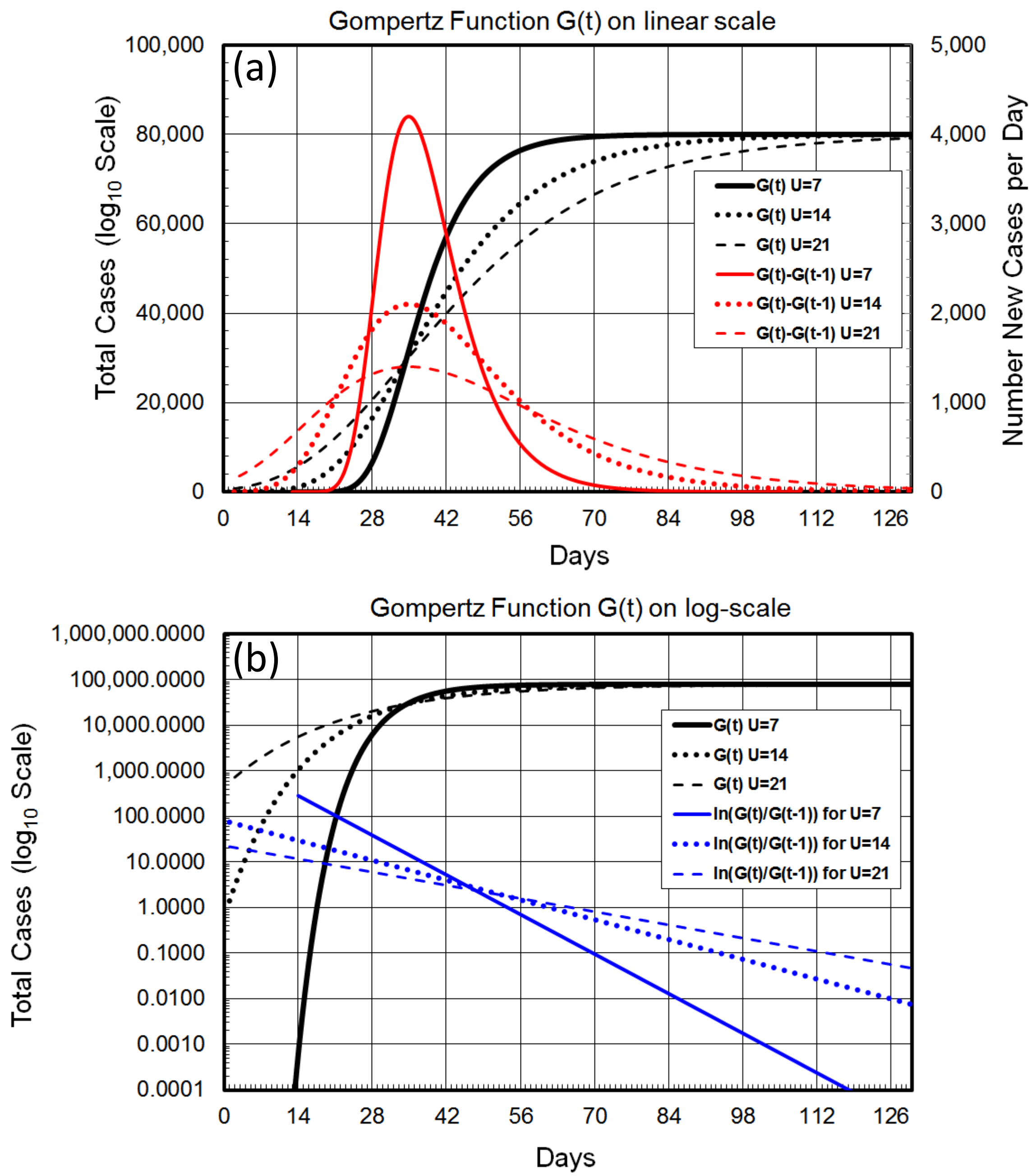

Fig. S2: Showing how the line $Y(t)=ln[ln[N/X(t)]]$ varies for different values of N. The straightness of the line is measured by the correlation coefficient between $Y(t)$ and t. The value of the correlation coefficient varies smoothly as value of N is changed

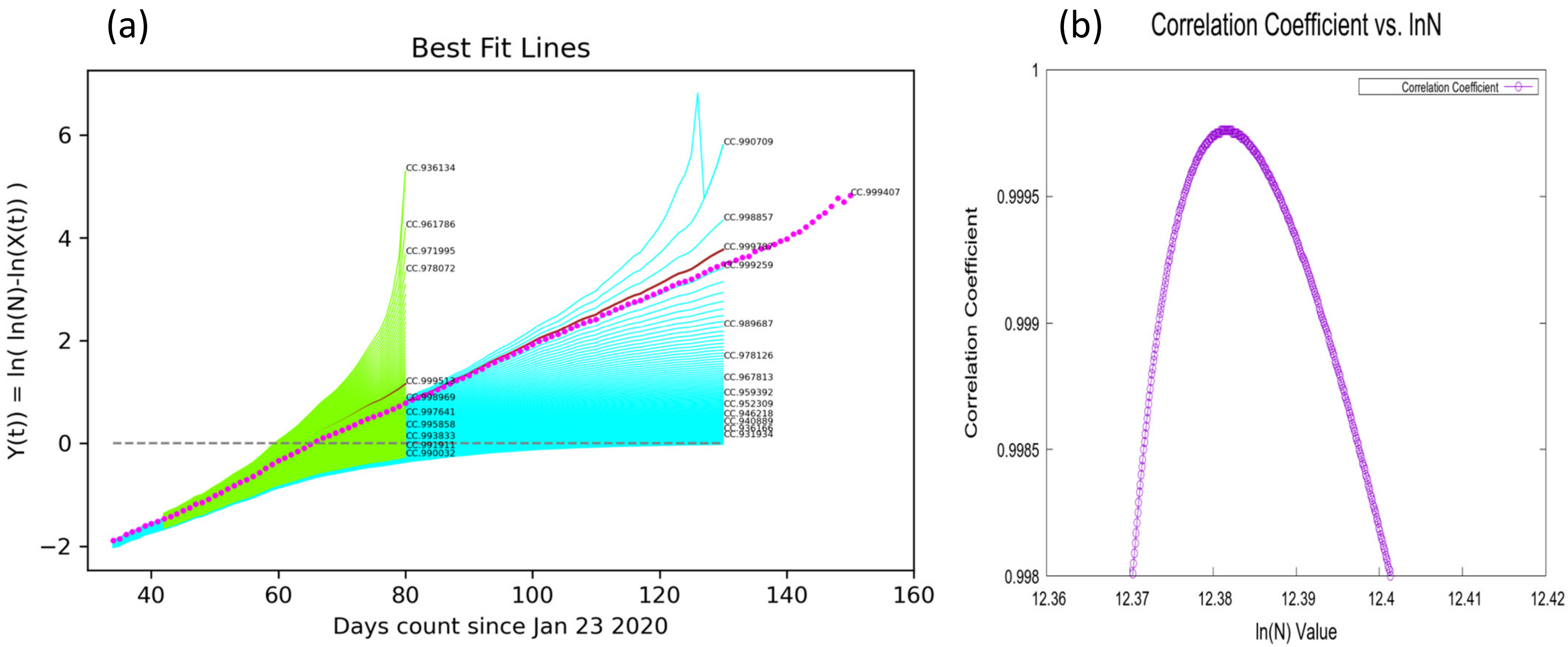

Fig S3. Showing five levels of smoothing on our standard four panel plots.

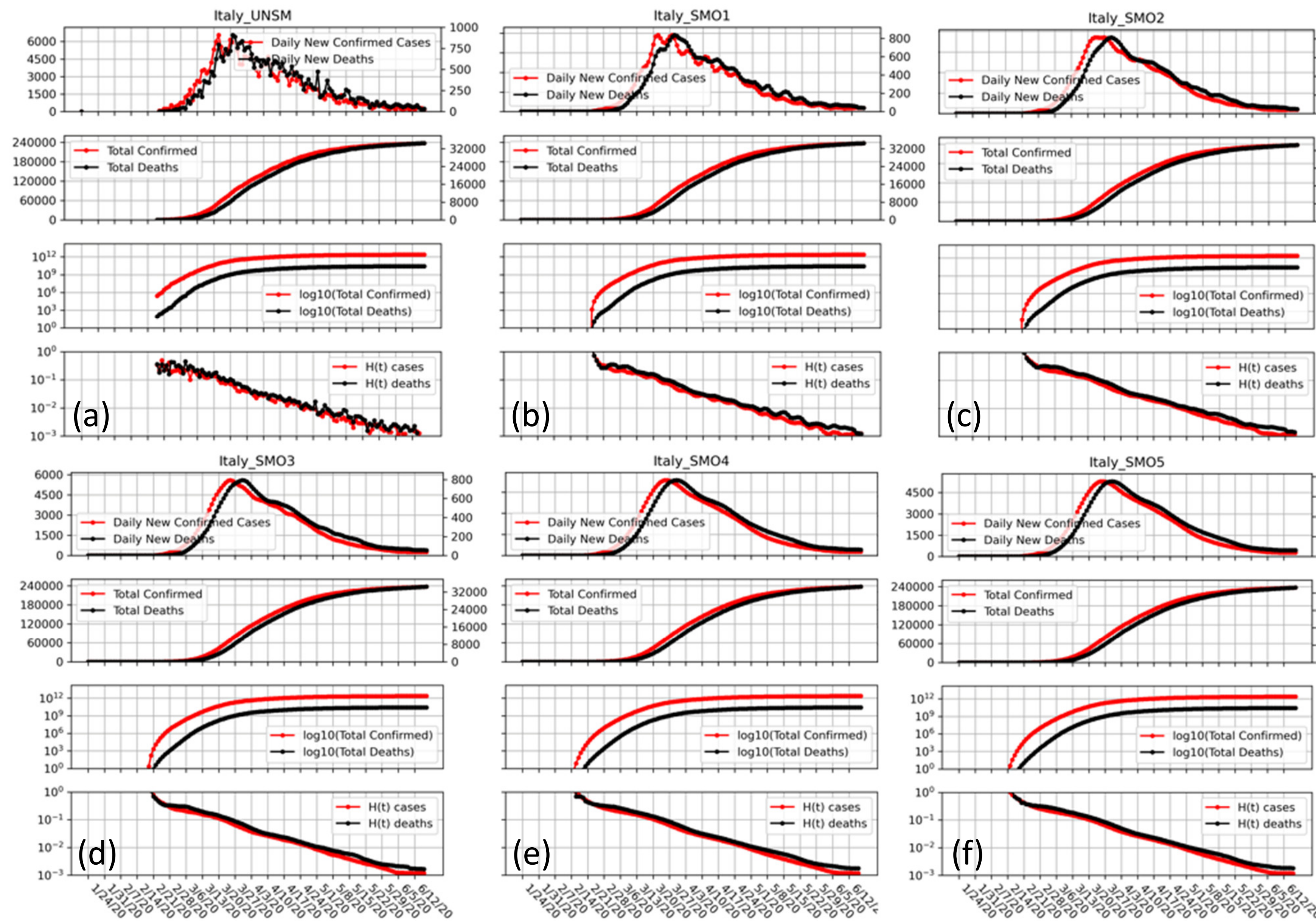

Table 1: Classification of Selected Locations (LOWESS smoothing SMO5 used to find peaks). KEY: 'c' means New Cases peaked, 'C' means at least halfway down this peak, 'd', 'D' are same for New Deaths. We also give Day of Peak, Day Halfway Up, and Day Halfway Down. Day Peak Confirmed is defined as (Day of Peak + Day Halfway Down)/2.

Country or Region of County	Classification Code	Number Confirmed Cases	Day Cases Halfway Up	Day New Cases Peak	Day Cases Peak Confirmed	Day Cases Halfway Down	Number Deaths	Day Deaths Halfway Up	Day New Deaths Peak	Day Deaths Peak Confirmed	Day Deaths Halfway Down	Deaths per Case
China_non_Hubei	cCdD	16518	1	12	16	21	128	14	22	27	32	0.8%
China	cCdD	84653	6	15	20	25	4640	11	24	30	36	5.5%
China_Hubei	cCdD	68135	7	16	21	26	4512	11	24	30	36	6.6%
Korea_South	cCdD	12535	33	40	44	48	281	39	63	73	84	2.2%
Italy	cCdD	238833	51	63	77	92	34675	54	67	80	94	14.5%
Norway	cCdD	8772	51	65	71	78	248	66	76	84	93	2.8%
Malaysia	cCdD	8590	53	69	78	87	121	59	68	77	86	1.4%
Switzerland	cCdD	31332	54	64	72	80	1956	63	74	84	95	6.2%
Greece	cCdD	3302	54	68	74	81	190	60	70	82	94	5.8%
Austria	cCdD	17408	56	64	69	75	693	64	76	86	96	4.0%
Luxembourg	cCdD	4133	56	65	71	77	110	63	76	82	88	2.7%
Thailand	cCdD	3156	56	66	72	78	58	66	76	81	87	1.8%
Australia	cCdD	7521	57	65	69	74	103	67	74	79	84	1.4%
Spain	cCdD	246752	57	68	77	87	28325	60	70	80	90	11.5%
Germany	cCdD	192480	57	69	76	84	8914	68	86	94	103	4.6%
Czechia	cCdD	10650	58	69	76	84	339	67	76	84	93	3.2%
Iran	cCdD	209970	58	69	78	88	9863	49	69	85	101	4.7%
France	cCdD	191730	58	70	80	90	29652	66	77	85	93	15.5%
Finland	cCdD	7155	59	77	94	112	327	82	91	99	107	4.6%
Netherlands	cCdD	49722	59	79	87	96	6095	63	74	88	102	12.3%
Israel	cCdD	21512	61	71	80	90	308	70	82	89	96	1.4%
Portugal	cCdD	39737	61	73	84	95	1540	65	81	92	104	3.9%
Belgium	cCdD	60810	61	79	88	97	9713	71	82	89	97	16.0%
Denmark	cCdD	12561	63	74	87	101	603	64	75	89	103	4.8%
Romania	cCdD	24505	64	82	102	122	1539	69	102	111	121	6.3%
United_Kingdom	cCdD	306210	65	85	102	120	42927	69	82	95	109	14.0%
Canada	cCdD	103767	67	91	109	128	8512	80	102	117	133	8.2%
Ecuador	cCdD	51643	68	81	92	104	4274	94	105	114	123	8.3%
Hungary	cCdD	4107	69	83	94	105	573	75	89	101	113	14.0%
Turkey	cCdD	190165	69	83	92	101	5001	71	88	97	107	2.6%
Serbia	cCdD	13092	71	84	92	101	263	66	89	99	109	2.0%
Algeria	cCdD	12076	71	117	97	77	861	68	77	82	88	7.1%
Ireland	cCdD	25391	72	83	90	98	1720	74	88	95	103	6.8%
Japan	cCdD	17879	73	84	90	97	965	81	97	112	127	5.4%
Morocco	cCdD	10344	74	89	103	118	214	65	75	81	87	2.1%
Sweden	cCdD	60837	81	146	130	115	5161	72	89	109	130	8.5%
United_Arab_Emirates	cCdD	45683	86	120	133	146	305	90	104	109	115	0.7%
Tajikistan	cCdD	5567	110	120	127	134	52	103	111	115	120	0.9%
Diamond_Princess	cCd=	712	18	25	28	32	13	27	35	31	27	1.8%
US	c=dD	2347022	60	67	-	-	121228	70	85	104	123	5.2%
Poland	c=dD	32527	66	140	-	-	1375	73	93	106	119	4.2%
Congo_Kinshasa	c=dD	6027	113	132	-	-	135	109	149	133	117	2.2%
Bosnia_and_Herzegovina	==dD	3409	64	74	-	-	172	70	108	91	75	5.0%
Dominican_Republic	==dD	26355	100	125	-	-	675	67	83	98	114	2.6%
Indonesia	==dD	44724	114	124	-	-	2535	78	148	120	92	5.7%
Cameroon	==dD	11331	116	135	-	-	313	87	107	99	91	2.8%

Philippines	==dD	29997	122	133	-	-	1186	69	82	100	118	4.0%
Cote_d_Ivoire	==dD	7021	137	112	-	-	58	85	148	119	91	0.8%
Belarus	c=d=	59487	86	115	-	-	357	81	148	-	-	0.6%
Russia	c=d=	598878	92	109	-	-	8349	103	132	-	-	1.4%
Kuwait	c=d=	41033	104	117	-	-	334	106	130	-	-	0.8%
Qatar	c=d=	89579	104	129	-	-	99	122	148	-	-	0.1%
Sudan	c=d=	8889	105	123	-	-	548	120	130	-	-	6.2%
Afghanistan	c=d=	29481	113	134	-	-	618	129	142	-	-	2.1%
Armenia	c=d=	21006	118	142	-	-	372	124	147	-	-	1.8%
Haiti	c=d=	5324	121	134	-	-	89	123	145	-	-	1.7%
Ethiopia	c=d=	4848	128	147	-	-	75	133	141	-	-	1.5%
North_Macedonia	c=d=	5311	131	147	-	-	251	137	148	-	-	4.7%
Peru	c===	260810	101	129	-	-	7820	110	55	-	-	3.0%
Chile	c===	250767	116	141	-	-	4035	130	147	-	-	1.6%
Egypt	c===	58141	122	148	-	-	2124	136	101	-	-	3.7%
Pakistan	c===	188926	128	145	-	-	3417	128	54	-	-	1.8%
WholeWorld	==d=	10583998	63	69	-	-	609543	65	82	-	-	5.8%
Ukraine	==d=	36643	86	103	-	-	1045	84	114	-	-	2.9%
Senegal	==d=	5705	95	147	-	-	89	138	146	-	-	1.6%
Bahrain	==d=	21513	110	116	-	-	67	136	148	-	-	0.3%
El_Salvador	==d=	4586	111	126	-	-	113	136	148	-	-	2.5%
Kazakhstan	==d=	17537	114	126	-	-	134	138	148	-	-	0.8%
India	==d=	417196	123	16	-	-	14476	123	146	-	-	3.5%
Bangladesh	==d=	108913	123	61	-	-	1545	121	147	-	-	1.4%
Nigeria	==d=	19649	123	73	-	-	533	100	149	-	-	2.7%
Guatemala	==d=	13090	124	64	-	-	582	129	139	-	-	4.4%
Kenya	==d=	4515	124	73	-	-	128	105	147	-	-	2.8%
Oman	==d=	29434	126	90	-	-	140	126	149	-	-	0.5%
South_Africa	==d=	94537	131	64	-	-	2102	127	149	-	-	2.2%
Argentina	==d=	42354	131	96	-	-	1078	127	148	-	-	2.5%
Mauritania	==d=	2823	135	66	-	-	114	127	139	-	-	4.0%
Bulgaria	====	3856	88	148	-	-	198	73	147	-	-	5.1%
Ghana	====	13588	100	107	-	-	83	141	148	-	-	0.6%
Saudi_Arabia	====	151974	111	118	-	-	1223	129	89	-	-	0.8%
Mexico	====	177175	116	40	-	-	21512	119	54	-	-	12.1%
Brazil	====	1058432	117	30	-	-	49624	104	146	-	-	4.7%
Bolivia	====	23865	124	50	-	-	771	126	87	-	-	3.2%
Azerbaijan	====	12529	127	77	-	-	152	128	147	-	-	1.2%
Panama	====	25162	128	95	-	-	507	76	147	-	-	2.0%
Moldova	====	13707	128	117	-	-	462	100	147	-	-	3.4%
Colombia	====	66449	130	37	-	-	2274	131	107	-	-	3.4%
Iraq	====	30056	134	72	-	-	1054	139	66	-	-	3.5%
Honduras	====	12383	138	125	-	-	378	108	140	-	-	3.1%
Canada_Quebec	cCdD	54884	68	102	114	126	5424	81	105	120	135	9.9%
Canada_Ontario	cCdD	35657	70	88	113	138	2676	79	100	109	118	7.5%
Canada_Alberta	cCdD	7781	82	93	98	103	153	70	100	105	111	2.0%
Italy_Marche	cCdD	6775	48	59	70	82	994	55	67	75	83	14.7%
Italy_Lombardia	cCdD	93173	48	61	74	88	16579	53	65	75	86	17.8%
Italy_Veneto	cCdD	19250	51	64	77	90	2004	58	71	92	114	10.4%
Italy_Friuli_Venezia_Giulia	cCdD	3305	52	64	74	84	344	54	69	84	100	10.4%
Italy_P.A._Trento_P_A_Trento	cCd=	4465	52	74	84	95	466	59	69	80	92	10.4%
Italy_Liguria	cCdD	9939	53	65	83	102	1553	55	67	83	100	15.6%
Italy_Toscana	cCdD	10217	53	66	77	89	1100	58	81	91	102	10.8%
Italy_Abruzzo	cCdD	3282	54	64	78	92	460	58	69	84	99	14.0%
Italy_Puglia	cCdD	4529	54	67	79	92	542	62	73	84	96	12.0%
Italy_Lazio	cCdD	8033	54	66	78	91	832	58	99	113	128	10.4%
Italy_Piemonte	cCdD	31254	55	82	91	101	4059	61	83	92	101	13.0%
Italy_Sicilia	cCdD	3073	56	64	73	82	280	60	68	79	91	9.1%
Italy_Campania	cCdD	4634	57	70	76	82	431	58	68	80	92	9.3%
US_Washington_King	cCdD	9366	56	75	89	104	604	57	74	89	105	6.4%
US_Washington_Snohomish	cCdD	3329	56	68	75	83	164	62	75	83	92	4.9%
US_New_York_Westchester	cCdD	34581	58	67	81	96	1416	72	79	89	99	4.1%

US_California_Santa_Clara	cCdD	3727	59	69	78	88	154	62	87	96	105	4.1%
US_New_York_NYC	cCdD	213056	61	78	88	98	22343	67	77	84	92	10.5%
US_New_York_Nassau	cCdD	41544	63	76	84	92	2179	72	79	87	96	5.2%
US_New_York_Rockland	cCdD	13529	63	73	84	95	667	71	79	89	99	4.9%
US_Louisiana_Orleans	cCdD	7571	64	72	76	80	529	62	79	89	99	7.0%
US_Michigan_Oakland	cCdD	11791	64	75	82	90	1081	68	81	95	110	9.2%
US_Michigan_Wayne	cCdD	22245	64	73	80	88	2690	70	91	98	105	12.1%
US_Missouri_St._Louis_St_Louis	cCdD	5941	64	75	99	123	555	76	95	107	119	9.3%
US_Indiana_Marion	cCdD	10977	65	102	115	128	669	73	98	113	129	6.1%
US_New_Jersey_Bergen	cCdD	19069	65	74	84	94	1706	71	82	94	107	8.9%
US_New_Jersey_Monmouth	cCdD	8998	65	75	86	98	700	71	85	107	130	7.8%
US_New_Jersey_Ocean	cCdD	9466	65	75	90	105	860	72	98	109	121	9.1%
US_New_York_Orange	cCdD	10666	65	77	88	99	473	70	78	91	105	4.4%
US_New_York_Suffolk	cCdD	41056	65	75	84	94	1970	71	80	96	113	4.8%
US_Connecticut_Fairfield	cCdD	16522	66	88	96	105	1367	75	88	99	111	8.3%
US_Louisiana_Jefferson	cCdD	8888	66	74	78	82	479	66	81	89	98	5.4%
US_Michigan_Macomb	cCdD	7175	66	75	85	96	898	72	83	93	103	12.5%
US_New_Jersey_Essex	cCdD	18592	66	78	89	100	1765	71	86	96	107	9.5%
US_New_Jersey_Morris	cCdD	6727	66	76	86	96	642	71	82	96	111	9.5%
US_New_York_Dutchess	cCdD	4150	66	75	87	99	151	102	109	112	115	3.6%
US_Pennsylvania_Northampton	cCdD	3327	66	75	92	109	255	93	103	108	113	7.7%
US_Louisiana_East_Baton_Rouge	cCdD	4514	67	76	82	88	265	73	94	106	118	5.9%
US_New_Jersey_Hudson	cCdD	19316	67	78	91	105	1308	78	86	91	96	6.8%
US_New_Jersey_Passaic	cCdD	16794	67	91	98	105	1019	80	96	103	110	6.1%
US_New_York_Erie	cCdD	7073	67	99	116	133	632	78	103	118	133	8.9%
US_New_York_Monroe	cCdD	3540	67	117	126	136	259	71	93	115	138	7.3%
US_Pennsylvania_Lehigh	cCdD	4109	67	75	84	93	281	93	118	123	128	6.8%
US_Pennsylvania_Montgomery	cCdD	8159	67	79	107	135	787	83	102	107	112	9.6%
US_New_Jersey_Middlesex	cCdD	16640	68	78	92	106	1104	73	100	108	116	6.6%
US_New_Jersey_Somerset	cCdD	4818	68	79	92	105	441	74	90	100	110	9.2%
US_New_Jersey_Union	cCdD	16341	68	82	90	98	1139	75	91	101	112	7.0%
US_Pennsylvania_Philadelphia	cCdD	25335	68	94	105	116	1564	77	103	114	126	6.2%
US_Colorado_Arapahoe	cCdD	4993	69	97	114	131	342	82	114	107	101	6.8%
US_Massachusetts_Hampden	cCdD	6620	69	93	107	121	649	77	91	100	110	9.8%
US_Massachusetts_Norfolk	cCdD	9042	69	91	99	108	919	81	93	101	110	10.2%
US_Illinois_Will	cCdD	6433	70	103	116	130	310	73	80	99	119	4.8%
US_Pennsylvania_Delaware	cCdD	7065	70	82	102	123	637	91	103	108	113	9.0%
US_Delaware_New_Castle	cCdD	4697	71	122	129	137	239	84	115	123	131	5.1%
US_District_of_Columbia	cCdD	10094	71	103	116	130	537	81	96	110	124	5.3%
US_Indiana_Lake	cCdD	4489	71	98	119	140	238	77	102	121	141	5.3%
US_Massachusetts_Suffolk	cCdD	19601	71	91	98	106	976	82	95	102	110	5.0%
US_New_Jersey_Burlington	cCdD	5056	71	96	106	116	372	84	102	111	121	7.4%
US_Pennsylvania_Bucks	cCdD	5580	71	94	107	120	555	86	102	110	118	9.9%
US_Connecticut_New_Haven	cCdD	12225	72	84	98	113	1065	77	91	107	123	8.7%
US_New_Jersey_Mercer	cCdD	7560	72	99	111	123	530	78	106	114	122	7.0%
US_Colorado_Adams	cCdD	3941	73	102	120	138	154	72	91	115	140	3.9%
US_Colorado_Denver	cCdD	6700	73	98	116	134	369	77	114	119	125	5.5%
US_Massachusetts_Essex	cCdD	15885	73	94	105	117	1081	81	98	110	122	6.8%
US_Massachusetts_Middlesex	cCdD	23647	73	90	101	112	1812	83	97	106	116	7.7%
US_Massachusetts_Plymouth	cCdD	8604	73	94	103	113	647	83	97	107	118	7.5%
US_New_Jersey_Camden	cCdD	7163	73	101	113	125	421	80	107	124	142	5.9%
US_Connecticut_Hartford	cCdD	11443	74	87	106	125	1352	80	91	105	119	11.8%
US_Pennsylvania_Berks	cCdD	4444	74	84	96	109	345	84	117	105	94	7.8%
US_Illinois_Cook	cCdD	87784	75	101	115	129	4439	77	109	123	138	5.1%
US_Massachusetts_Worcester	cCdD	12192	76	98	111	124	905	88	110	121	132	7.4%
US_South_Dakota_Minnehaha	cCdD	3537	77	85	99	113	55	96	106	111	117	1.6%
US_Maryland_Montgomery	cCdD	14204	78	118	129	141	725	85	98	114	131	5.1%
US_Maryland_Prince_Georges_Prince_George_s	cCdD	18080	78	102	119	136	661	83	100	119	139	3.7%
US_Maryland_Baltimore_City	cCdD	7148	79	123	133	143	319	82	103	120	138	4.5%
US_Delaware_Sussex	cCdD	4509	81	95	107	119	176	82	109	115	121	3.9%
US_Kentucky_Jefferson	cCdD	3651	82	133	118	103	185	74	84	94	104	5.1%
US_Michigan_Michigan_Department_Corrections_	cCdD	4097	84	118	124	130	68	80	92	99	107	1.7%
US_Illinois_DuPage	cCdD	8736	87	114	121	129	455	80	103	120	137	5.2%
US_Michigan_Kent	cCdD	4628	87	98	114	130	128	82	131	106	82	2.8%

US_Virginia_Fairfax	cCdD	13579	87	124	131	139	445	89	99	115	131	3.3%
US_Virginia_Prince_William	cCdD	6962	90	123	130	138	134	90	109	121	133	1.9%
US_Iowa_Polk	cCdD	5582	93	103	121	140	168	93	123	132	142	3.0%
US_Minnesota_Hennepin	cCdD	10988	99	119	129	140	751	87	103	119	136	6.8%
US_Virginia_Loudoun	cCdD	3632	112	125	134	143	84	99	110	114	119	2.3%
US_Georgia_Fulton	cCd=	5885	64	80	96	113	304	70	126	-	-	5.2%
US_Illinois_Lake	cCd=	9404	77	108	119	130	405	77	131	-	-	4.3%
US_Massachusetts_Bristol	cCd=	8081	84	96	110	125	548	81	102	-	-	6.8%
US_New_Mexico_McKinley	cCd=	3155	84	100	121	142	161	101	111	-	-	5.1%
US_Illinois_Kane	cCd=	7457	96	112	120	129	254	98	118	-	-	3.4%
US_Georgia_Cobb	c=dD	4134	67	104	-	-	234	70	127	99	71	5.7%
US_Pennsylvania_Lancaster	c=dD	4106	69	88	-	-	350	81	92	102	112	8.5%
US_Alabama_Mobile	c=dD	3052	72	148	-	-	132	82	103	109	116	4.3%
US_Pennsylvania_Chester	c=dD	3537	72	99	-	-	317	84	106	117	128	9.0%
US_Maryland_Anne_Arundel	c=dD	4946	73	129	-	-	201	77	95	113	132	4.1%
US_New_Hampshire_Hillsborough	c=dD	3145	82	125	-	-	224	120	130	136	143	7.1%
US_Wisconsin_Milwaukee	c=dD	10406	106	125	-	-	373	71	79	98	117	3.6%
US_Washington_Yakima	c=dD	6435	108	136	-	-	142	74	147	119	91	2.2%
US_Puerto_Rico	c=dD	6685	118	136	-	-	149	70	80	97	114	2.2%
US_North_Carolina_Durham	c=dD	3244	122	142	-	-	60	88	97	106	116	1.8%
US_South_Carolina_Greenville	c=dD	3822	131	147	-	-	75	91	97	100	104	2.0%
US_Florida_Broward	==dD	10920	70	78	-	-	377	70	90	102	114	3.5%
US_Nevada_Clark	==dD	10093	71	74	-	-	400	69	82	103	124	4.0%
US_California_Alameda	==dD	4999	76	130	-	-	121	74	83	101	120	2.4%
US_Tennessee_Davidson	==dD	7466	87	97	-	-	98	75	139	109	80	1.3%
US_Ohio_Hamilton	==dD	3836	93	102	-	-	188	77	130	134	138	4.9%
US_California_Tulare	==dD	3211	100	108	-	-	116	86	115	108	101	3.6%
US_Georgia_Gwinnett	==dD	6225	100	131	-	-	163	78	105	99	93	2.6%
US_Alabama_Jefferson	==dD	2895	118	121	-	-	126	83	119	124	130	4.4%
US_Tennessee_Shelby	==dD	7796	118	99	-	-	166	72	140	114	89	2.1%
US_California_San_Bernardino	==dD	9241	123	91	-	-	234	78	114	125	136	2.5%
US_North_Carolina_Mecklenburg	==dD	8377	124	148	-	-	143	79	132	118	105	1.7%
US_Florida_Collier	==dD	3110	126	75	-	-	65	85	116	127	139	2.1%
US_Texas_Fort_Bend	==dD	2915	134	103	-	-	50	75	105	108	112	1.7%
US_Arizona_Pima	==dD	5464	136	84	-	-	247	82	107	100	93	4.5%
US_Florida_Lee	==dD	3430	136	75	-	-	149	86	109	97	86	4.3%
US_Texas_Harris	==dD	22429	136	78	-	-	335	75	102	95	89	1.5%
US_Florida_Pinellas	==dD	3491	140	71	-	-	129	91	103	108	114	3.7%
US_Florida_Orange	==dD	4803	141	72	-	-	51	75	87	91	96	1.1%
US_Florida_Duval	==dD	2876	142	74	-	-	62	67	122	99	77	2.2%
US_Ohio_Cuyahoga	c=d=	5820	64	120	-	-	341	82	137	-	-	5.9%
US_Georgia_DeKalb	c=d=	5042	68	124	-	-	166	84	144	-	-	3.3%
US_Maryland_Baltimore	c=d=	7635	71	115	-	-	458	89	116	-	-	6.0%
US_Ohio_Franklin	c=d=	8029	87	103	-	-	370	98	116	-	-	4.6%
US_Nebraska_Douglas	c=d=	6461	101	128	-	-	83	132	139	-	-	1.3%
US_Minnesota_Ramsey	c=d=	4394	105	121	-	-	213	109	139	-	-	4.8%
US_Arizona_Navajo	c=d=	3166	106	144	-	-	97	98	141	-	-	3.1%
US_Alabama_Montgomery	c=d=	3307	117	141	-	-	85	118	140	-	-	2.6%
US_California_Kern	c=d=	4049	119	149	-	-	60	101	129	-	-	1.5%
US_California_Imperial	c=d=	5270	128	139	-	-	68	135	146	-	-	1.3%
US_California_San_Diego	==d=	10738	72	109	-	-	341	75	109	-	-	3.2%
US_California_Los_Angeles	==d=	83831	88	132	-	-	3171	77	93	-	-	3.8%
US_Texas_Dallas	==d=	16645	101	108	-	-	324	80	116	-	-	1.9%
US_Texas_Tarrant	==d=	8759	103	110	-	-	211	76	108	-	-	2.4%
US_Texas_El_Paso	==d=	4427	105	136	-	-	122	101	128	-	-	2.8%
US_California_Orange	==d=	10046	109	75	-	-	273	115	147	-	-	2.7%
US_Arizona_Yuma	==d=	4388	130	69	-	-	69	130	147	-	-	1.6%
US_Florida_Palm_Beach	==d=	10375	130	115	-	-	476	69	143	-	-	4.6%
US_California_Fresno	==d=	3365	131	112	-	-	70	116	149	-	-	2.1%
US_California_Riverside	==d=	13409	131	86	-	-	431	80	97	-	-	3.2%
US_Texas_Travis	==d=	5802	137	103	-	-	112	81	98	-	-	1.9%
US_Arizona_Maricopa	==d=	29446	139	108	-	-	663	98	109	-	-	2.3%
US_Florida_Hillsborough	==d=	5425	140	73	-	-	119	103	116	-	-	2.2%
US_Texas_Bexar	==d=	6292	140	79	-	-	97	71	82	-	-	1.5%

Table 2: Comparing Best Line (BL) and Peak Detection (PD) Prediction of Plateau N Value.

Type	Location	Class	Maximum Value Today	BL N-Prediction Today	%SD of N Plateau	Days at Plateau	Day of BL Prediction	Day of PD Prediction	BL N-Prediction Then	PD N-Prediction Then	% Error BL Prediction	% Error DM Prediction	BL or DM Better?
Cases	China	cC	84572	85924	0.00	132	14	20	98422	103778	16.4	22.7	BL
Cases	China_Hubei	cC	68135	69197	0.51	98	14	21	74259	89953	9.0	32.0	BL
Cases	China_non_Hubei	cC	16437	16376	5.21	106	14	16	15445	17073	6.0	3.9	PD
Cases	Thailand	cC	3148	3198	0.00	82	70	72	3081	3468	2.1	10.2	BL
Cases	Japan	cC	17780	18064	0.00	57	93	90	19378	22520	9.0	26.7	BL
Cases	Australia	cC	7474	7172	6.78	85	66	69	7869	8665	5.3	15.9	BL
Cases	Germany	cC	191272	194331	0.00	83	68	76	208464	198918	9.0	4.0	PD
Cases	Malaysia	cC	8572	8891	2.10	46	106	78	7125	7600	16.9	11.3	PD
Cases	Diamond_Princess	cC	712	719	0.57	25	127	28	723	1041	1.5	46.2	BL
Cases	France	cC	191117	194075	0.14	73	79	80	180052	187814	5.8	1.7	PD
Cases	Iran	cC	204952	281110	9.42	12	138	78	246090	120251	20.1	41.3	BL
Cases	Italy	cC	238499	241872	0.39	72	80	77	198256	203093	16.9	14.8	PD
Cases	Italy_Lombardia	cC	92968	94454	0.00	70	64	74	87585	77867	5.8	16.2	BL
Cases	Italy_Veneto	cC	19245	19552	0.00	80	72	77	17445	18780	9.4	2.4	PD
Cases	United_Kingdom	cC	304331	320393	0.04	52	100	102	264224	282220	13.2	7.3	PD
Cases	Canada	cC	103078	112170	1.50	48	104	109	93302	111805	9.5	8.5	PD
Cases	Italy_Liguria	cC	9927	10085	0.00	69	62	83	8985	7246	9.5	27.0	BL
Cases	Spain	cC	246272	250211	0.00	76	76	77	268408	240035	9.0	2.5	PD
Cases	Italy_Piemonte	cC	31241	31740	0.00	69	83	91	27277	46594	12.7	49.1	BL
Cases	Canada_Ontario	cC	35217	38549	1.10	30	122	112	31876	31105	9.5	11.7	BL
Cases	Italy_Campania	cC	4617	4809	1.46	69	80	76	4061	6241	12.0	35.2	BL
Cases	Italy_Marche	cC	6768	6876	0.00	84	61	70	6036	5874	10.8	13.2	BL
Cases	Italy_Toscana	cC	10210	10373	0.00	84	68	77	9189	10362	10.0	1.5	PD
Cases	Norway	cC	8745	8884	0.00	85	67	71	7915	9957	9.5	13.9	BL
Cases	Switzerland	cC	31292	31792	0.00	79	71	72	26465	31956	15.4	2.1	PD
Cases	Austria	cC	17341	16613	6.60	82	69	69	15055	18068	13.2	4.2	PD
Cases	Netherlands	cC	49593	48376	4.04	71	81	87	44889	62504	9.5	26.0	BL
Cases	US_Washington_King	cC	9211	9125	2.36	72	79	89	8337	9138	9.5	0.8	PD
Cases	Belgium	cC	60550	61421	0.26	67	85	88	54807	71749	9.5	18.5	BL
Cases	Italy_Friuli_Venezia_Giulia	cC	3305	3357	0.00	92	60	74	3235	3270	2.1	1.1	PD
Cases	Italy_Lazio	cC	8017	8145	0.00	74	64	78	7853	6760	2.0	15.7	BL
Cases	US_California_Santa_Clara	cC	3547	3118	9.89	42	110	78	2555	2375	28.0	33.0	BL
Cases	Algeria	cC	11771	14568	0.00	33	119	97	12403	19598	5.4	66.5	BL
Cases	Italy_Sicilia	cC	3072	3464	0.79	71	81	73	2806	2859	8.7	6.9	PD
Cases	Finland	cC	7143	7509	3.30	61	91	94	6201	6561	13.2	8.1	PD
Cases	Italy_Puglia	cC	4527	4599	0.00	82	69	79	4103	4275	9.4	5.6	PD
Cases	US_New_York_Westchester	cC	34521	35052	0.14	63	89	81	28972	22523	16.1	34.8	BL
Cases	US_Washington_Snohomish	cC	3237	3321	2.87	51	101	75	2690	2965	16.9	8.4	PD
Cases	Denmark	cC	12391	12587	0.87	59	93	87	10300	11813	16.9	4.7	PD
Cases	Ireland	cC	25379	25630	5.04	49	103	90	24674	30746	2.8	21.1	BL
Cases	US_New_York_NYC	cC	212446	215935	0.43	62	90	88	176049	237634	17.1	11.9	PD
Cases	Italy_Abruzzo	cC	3281	3319	0.54	71	81	78	2848	2557	13.2	22.1	BL
Cases	Italy_P.A._Trento_P_A_Trento	cC	4463	4534	0.00	72	80	84	4039	6241	9.5	39.8	BL
Cases	Romania	cC	24045	22183	7.07	52	99	102	18278	18062	24.0	24.9	BL
Cases	US_New_York_Nassau	cC	41479	42079	0.21	72	79	84	38790	46547	6.5	12.2	BL
Cases	US_Illinois_Cook	cC	87177	99270	6.23	41	110	115	85350	109201	2.1	25.3	BL
Cases	US_Massachusetts_Middlesex	cC	23574	23978	0.24	63	81	101	25692	27036	9.0	14.7	BL
Cases	Canada_Alberta	cC	7704	7827	0.00	45	107	98	6404	10720	16.9	39.1	BL
Cases	Hungary	cC	4094	4241	1.41	53	99	94	4915	4074	20.1	0.5	PD
Cases	Serbia	cC	12894	11884	6.82	59	76	92	13100	13265	1.6	2.9	BL
Cases	US_Massachusetts_Norfolk	cC	8994	9137	0.00	58	93	99	10799	12237	20.1	36.1	BL
Cases	US_Massachusetts_Suffolk	cC	19551	19920	8.39	62	88	98	19141	25935	2.1	32.7	BL
Cases	US_New_Jersey_Bergen	cC	19010	19294	0.23	63	89	84	16374	16459	13.9	13.4	PD
Cases	Luxembourg	cC	4120	4185	0.00	79	73	71	3732	4308	9.4	4.6	PD

Cases	US_Louisiana_Orleans	cC	7518	8193	0.00	51	101	76	6804	8948	9.5	19.0	BL
Cases	US_New_York_Suffolk	cC	40972	41422	0.65	69	82	84	39733	38607	3.0	5.8	BL
Cases	US_Pennsylvania_Montgomery	cC	8103	9371	8.07	29	123	107	7689	4930	5.1	39.2	BL
Cases	Canada_Quebec	cC	54766	57803	1.81	44	108	114	48524	84353	11.4	54.0	BL
Cases	US_Colorado_Denver	cC	6630	7470	0.00	44	107	116	6244	7883	5.8	18.9	BL
Cases	US_Connecticut_Fairfield	cC	16475	16793	0.59	64	78	96	14391	21768	12.6	32.1	BL
Cases	US_Georgia_Fulton	cC	5496	5609	3.48	28	124	96	4568	4009	16.9	27.1	BL
Cases	US_Louisiana_Jefferson	cC	8681	9041	8.62	39	107	78	7536	8298	13.2	4.4	PD
Cases	US_Michigan_Oakland	cC	11685	12085	6.99	40	112	82	9713	9916	16.9	15.1	PD
Cases	US_Colorado_Arapahoe	cC	4941	5390	0.99	46	106	114	4654	6252	5.8	26.5	BL
Cases	US_New_York_Rockland	cC	13504	13735	0.33	54	98	84	11889	12762	12.0	5.5	PD
Cases	Turkey	cC	187685	167702	8.36	66	86	92	136703	176867	27.2	5.8	PD
Cases	US_District_of_Columbia	cC	10020	11001	0.68	44	106	116	9439	13925	5.8	39.0	BL
Cases	US_Maryland_Montgomery	cC	14079	18786	6.92	32	120	129	20025	23621	42.2	67.8	BL
Cases	US_Michigan_Wayne	cC	22139	22493	0.00	53	99	80	18403	18381	16.9	17.0	BL
Cases	US_Minnesota_Hennepin	cC	10830	11793	7.00	18	134	129	11003	15964	1.6	47.4	BL
Cases	US_New_Jersey_Essex	cC	18551	18870	0.25	70	73	89	18718	16187	0.9	12.7	BL
Cases	US_New_Jersey_Hudson	cC	19280	19656	2.15	60	92	91	17451	15918	9.5	17.4	BL
Cases	US_New_Jersey_Middlesex	cC	16605	16851	0.31	59	93	92	14152	12224	14.8	26.4	BL
Cases	US_New_Jersey_Monmouth	cC	8942	9745	0.00	36	116	86	8754	6806	2.1	23.9	BL
Cases	US_New_York_Monroe	cC	3498	3796	0.54	25	119	126	4329	6254	23.8	78.8	BL
Cases	US_New_York_Orange	cC	10648	10741	0.84	69	83	88	9244	10859	13.2	2.0	PD
Cases	US_Delaware_New_Castle	cC	4647	4771	7.21	31	121	129	4206	8788	9.5	89.1	BL
Cases	US_Illinois_DuPage	cC	8682	9085	7.35	16	135	121	8666	15061	0.2	73.5	BL
Cases	US_New_Jersey_Union	cC	16322	16635	0.26	64	88	90	15980	18370	2.1	12.5	BL
Cases	US_New_York_Dutchess	cC	4138	4204	0.00	52	100	87	3439	3147	16.9	23.9	BL
Cases	US_New_York_Erie	cC	7004	8111	2.09	31	121	115	7633	8722	9.0	24.5	BL
Cases	US_Pennsylvania_Philadelphia	cC	24841	26366	0.34	47	105	105	21402	32502	13.8	30.8	BL
Cases	US_Virginia_Fairfax	cC	13419	19779	8.83	43	109	131	18095	25864	34.8	92.7	BL
Cases	US_Connecticut_Hartford	cC	11405	12329	1.31	51	91	106	13229	8807	16.0	22.8	BL
Cases	US_Illinois_Lake	cC	9326	9907	8.68	21	127	119	11542	13876	23.8	48.8	BL
Cases	US_Indiana_Marion	cC	10945	11883	4.21	35	117	115	9906	16540	9.5	51.1	BL
Cases	US_Massachusetts_Essex	cC	15829	16460	3.10	54	97	105	14073	19356	11.1	22.3	BL
Cases	US_New_Jersey_Mercer	cC	7541	7883	1.27	54	80	111	8178	10786	8.4	43.0	BL
Cases	US_New_Jersey_Morris	cC	6699	6803	0.39	75	74	86	6806	5912	1.6	11.7	BL
Cases	US_New_Jersey_Passaic	cC	16769	16995	0.46	58	94	98	15178	25589	9.5	52.6	BL
Cases	US_New_Jersey_Somerset	cC	4813	4889	0.00	68	83	92	5328	3917	10.7	18.6	BL
Cases	US_Pennsylvania_Delaware	cC	7038	7371	0.86	51	87	102	6110	4634	13.2	34.2	BL
Cases	US_Connecticut_New_Haven	cC	12185	12571	1.77	60	87	99	12656	11180	3.9	8.2	BL
Cases	US_Massachusetts_Worcester	cC	12130	12332	0.17	38	102	111	10979	14591	9.5	20.3	BL
Cases	US_Michigan_Macomb	cC	7152	7266	0.00	58	94	85	6209	5887	13.2	17.7	BL
Cases	US_New_Jersey_Burlington	cC	5023	5214	1.74	53	99	106	4361	6515	13.2	29.7	BL
Cases	US_New_Jersey_Camden	cC	7135	7626	1.69	49	103	113	6458	10318	9.5	44.6	BL
Cases	US_New_Jersey_Ocean	cC	9425	10118	1.56	46	104	90	8182	6398	13.2	32.1	BL
Cases	US_Pennsylvania_Bucks	cC	5547	5823	3.67	58	94	106	5020	6333	9.5	14.2	BL
Cases	US_Colorado_Adams	cC	3909	4733	2.10	32	120	120	3826	4841	2.1	23.8	BL
Cases	US_Kentucky_Jefferson	cC	3582	3561	5.13	18	130	118	3109	7317	13.2	104.3	BL
Cases	US_Maryland_Baltimore_City	cC	7053	7863	0.22	28	121	133	6384	12786	9.5	81.3	BL
Cases	US_Massachusetts_Plymouth	cC	8583	8731	0.25	54	96	103	7768	11308	9.5	31.7	BL
Cases	US_Michigan_Kent	cC	4590	5000	0.40	36	116	114	4154	4044	9.5	11.9	BL
Cases	US_Missouri_St._Louis_St_Louis	cC	5850	6505	3.68	32	120	98	5727	3098	2.1	47.0	BL
Cases	US_Illinois_Will	cC	6367	6845	1.37	37	115	117	5763	8538	9.5	34.1	BL
Cases	US_Louisiana_East_Baton_Rouge	cC	4374	5080	8.13	17	135	82	5575	2209	27.5	49.5	BL
Cases	US_Massachusetts_Bristol	cC	8035	8731	8.56	32	120	110	8505	8372	5.8	4.2	PD
Cases	US_Pennsylvania_Lehigh	cC	4085	4134	3.26	44	108	83	3395	2778	16.9	32.0	BL
Cases	US_Pennsylvania_Northampton	cC	3309	3415	1.99	45	107	92	2750	1886	16.9	43.0	BL
Cases	US_Delaware_Sussex	cC	4495	4554	0.65	42	107	106	5064	4433	12.7	1.4	PD
Cases	US_Illinois_Kane	cC	7399	7503	3.96	23	129	121	7790	10481	5.3	41.7	BL
Cases	US_Massachusetts_Hampden	cC	6598	6703	0.00	45	107	107	5728	8260	13.2	25.2	BL
Cases	US_Pennsylvania_Berks	cC	4407	4615	0.48	43	109	96	3988	3653	9.5	17.1	BL
Cases	US_Iowa_Polk	cC	5498	6384	2.84	27	124	121	5245	4349	4.6	20.9	BL
Cases	US_Indiana_Lake	cC	4400	5283	0.00	35	117	119	4307	4824	2.1	9.6	BL
Cases	US_South_Dakota_Minnehaha	cC	3523	3579	0.00	44	108	99	3709	2712	5.3	23.0	BL
Deaths	China	dD	4639	4713	0.00	113	22	30	5398	6121	16.4	31.9	BL
Deaths	China_Hubei	dD	4512	4565	0.63	53	21	30	4417	5942	2.1	31.7	BL
Deaths	China_non_Hubei	dD	127	128	4.44	122	28	27	133	163	4.7	28.3	BL

Deaths	Iran	dD	9623	8550	9.89	59	92	85	6932	7940	28.0	17.5	PD
Deaths	Italy	dD	34634	35242	0.41	71	69	80	29392	29159	15.1	15.8	BL
Deaths	Korea_South	dD	280	284	0.00	85	65	74	274	356	2.1	27.1	BL
Deaths	Italy_Lombardia	dD	16570	16819	0.18	83	60	75	18671	14822	12.7	10.5	PD
Deaths	US	dD	119977	126194	1.55	43	109	104	102469	94756	14.6	21.0	BL
Deaths	Italy_Veneto	dD	2002	2033	0.00	61	91	92	1707	1345	14.7	32.8	BL
Deaths	US_Washington_King	dD	600	611	1.05	60	92	90	565	568	5.8	5.3	PD
Deaths	France	dD	29574	30046	0.00	67	85	85	26769	29697	9.5	0.4	PD
Deaths	Spain	dD	28323	28189	3.81	60	83	80	23001	25731	18.8	9.2	PD
Deaths	Italy_Piemonte	dD	4051	4102	2.95	69	83	92	3966	5172	2.1	27.7	BL
Deaths	Italy_Marche	dD	994	1005	0.95	76	73	74	1030	984	3.6	1.0	PD
Deaths	Japan	dD	955	971	0.38	48	104	112	970	1100	1.6	15.2	BL
Deaths	Italy_Liguria	dD	1549	1578	1.03	59	93	83	1344	1016	13.2	34.4	BL
Deaths	Italy_Lazio	dD	827	911	6.11	39	113	114	748	1258	9.6	52.1	BL
Deaths	Switzerland	dD	1956	1987	0.00	67	81	84	1752	1929	10.4	1.4	PD
Deaths	Italy_Friuli_Venezia_Giulia	dD	344	347	0.29	73	73	85	362	326	5.2	5.2	PD
Deaths	Netherlands	dD	6090	6171	0.45	65	87	88	5287	4816	13.2	20.9	BL
Deaths	United_Kingdom	dD	42632	40774	6.54	58	94	95	35288	35720	17.2	16.2	PD
Deaths	Germany	dD	8895	9019	0.30	67	85	94	8708	11351	2.1	27.6	BL
Deaths	Italy_Puglia	dD	540	548	0.00	59	91	84	488	418	9.6	22.6	BL
Deaths	Philippines	dD	1169	1139	5.99	53	82	100	1273	818	8.9	30.0	BL
Deaths	US_New_York_NYC	dD	22278	22612	0.20	70	82	84	20223	21884	9.2	1.8	PD
Deaths	Italy_Toscana	dD	1095	1114	0.32	61	91	92	1112	1323	1.6	20.8	BL
Deaths	Belgium	dD	9696	9801	0.68	59	93	89	8776	10495	9.5	8.2	PD
Deaths	Italy_Abruzzo	dD	459	463	0.84	42	106	84	381	323	17.0	29.6	BL
Deaths	Italy_Campania	dD	431	437	0.00	62	88	80	358	345	16.9	20.0	BL
Deaths	Italy_P.A._Trento_P_A_Trento	dD	466	470	1.20	64	85	80	387	426	17.0	8.6	PD
Deaths	Sweden	dD	5111	5624	4.14	38	114	109	4626	4534	9.5	11.3	BL
Deaths	Canada	dD	8482	9249	0.48	49	103	117	8703	10421	2.6	22.9	BL
Deaths	Denmark	dD	600	609	0.23	63	88	89	491	505	18.2	15.8	PD
Deaths	Greece	dD	190	195	2.39	59	75	83	173	154	8.9	18.9	BL
Deaths	Portugal	dD	1530	1564	1.84	58	94	92	1384	1359	9.5	11.2	BL
Deaths	US_Louisiana_Orleans	dD	529	537	0.00	66	86	89	478	641	9.6	21.2	BL
Deaths	Austria	dD	690	665	2.52	61	69	86	700	731	1.4	5.9	BL
Deaths	Ecuador	dD	4223	3971	8.64	35	115	114	4290	4466	1.6	5.8	BL
Deaths	Turkey	dD	4950	5029	0.00	61	89	97	4751	5469	4.0	10.5	BL
Deaths	Italy_Sicilia	dD	280	278	1.59	64	88	80	232	209	17.1	25.4	BL
Deaths	Malaysia	dD	121	117	5.18	67	84	76	105	89	13.2	26.4	BL
Deaths	US_New_York_Suffolk	dD	1964	1994	1.21	43	109	96	2175	1228	10.7	37.5	BL
Deaths	US_Washington_Snohomish	dD	163	160	4.20	37	112	82	129	125	20.9	23.3	BL
Deaths	Norway	dD	244	236	4.54	61	85	85	220	279	9.8	14.3	BL
Deaths	US_California_Santa_Clara	dD	152	154	0.00	52	100	96	131	209	13.8	37.5	BL
Deaths	US_Michigan_Wayne	dD	2687	2730	0.20	63	80	97	2246	3609	16.4	34.3	BL
Deaths	Poland	dD	1356	1223	9.54	51	98	106	1077	1326	20.6	2.2	PD
Deaths	US_Connecticut_Fairfield	dD	1361	1386	0.53	56	93	99	1483	1296	9.0	4.8	PD
Deaths	US_Illinois_Cook	dD	4404	5095	0.76	35	117	123	4129	6292	6.2	42.9	BL
Deaths	US_Michigan_Oakland	dD	1077	1094	0.00	53	99	95	1014	926	5.8	14.0	BL
Deaths	US_New_York_Nassau	dD	2178	2212	0.00	56	96	87	1832	1794	15.9	17.6	BL
Deaths	Australia	dD	102	103	0.99	57	93	80	99	114	2.9	11.8	BL
Deaths	Canada_Ontario	dD	2657	2796	0.08	61	86	109	3092	3416	16.4	28.6	BL
Deaths	Ireland	dD	1715	1742	0.00	60	88	95	1742	2049	1.6	19.5	BL
Deaths	Morocco	dD	214	218	1.12	63	80	81	185	225	13.6	5.1	PD
Deaths	US_Louisiana_Jefferson	dD	477	484	1.10	65	85	90	449	554	5.9	16.1	BL
Deaths	US_Michigan_Macomb	dD	899	935	1.66	53	99	93	797	872	11.3	3.0	PD
Deaths	Canada_Quebec	dD	5417	5925	1.06	42	110	120	4903	6798	9.5	25.5	BL
Deaths	Dominican_Republic	dD	662	757	4.05	21	131	98	623	418	5.9	36.9	BL
Deaths	Israel	dD	306	310	0.00	65	86	89	344	315	12.4	2.9	PD
Deaths	Luxembourg	dD	110	112	2.16	57	78	82	107	122	2.7	10.9	BL
Deaths	Czechia	dD	336	338	2.12	48	104	85	279	293	17.0	12.8	PD
Deaths	Hungary	dD	570	596	0.66	56	89	100	621	502	8.9	11.9	BL
Deaths	US_New_Jersey_Bergen	dD	1696	1727	0.49	52	100	94	1597	1391	5.8	18.0	BL
Deaths	Finland	dD	326	328	3.19	43	107	99	322	385	1.2	18.1	BL
Deaths	US_Florida_Broward	dD	373	400	1.73	44	108	102	351	361	5.9	3.2	PD
Deaths	US_Nevada_Clark	dD	398	416	4.93	39	112	102	345	228	13.3	42.7	BL
Deaths	US_New_Jersey_Essex	dD	1760	1789	0.26	51	101	96	1527	1777	13.2	1.0	PD
Deaths	US_New_Jersey_Middlesex	dD	1101	1158	0.14	44	106	108	1037	1568	5.8	42.4	BL

Table 3: Forecasts of Plateau N Ordered by Size and Certainty (green shading more certain but may involves small increases to plateau so less important).

Cases or Deaths	Location	Total Number Now	Predicted Plateau N Now	%SD of Plateau	Difference Now to to Plateau	%Difference	Number Days at Plateau	Slope of Plateau with Day
Cases	Peru	257,447	478,018	1.3	220,571	85.7	22	19
Deaths	Brazil	51,271	97,987	3.6	46,716	91.1	16	42
Cases	Belarus	59,023	82,618	5.7	23,595	40.0	22	158
Cases	Indonesia	46,845	68,939	5.0	22,094	47.2	8	395
Cases	Afghanistan	29,157	45,900	7.4	16,743	57.4	10	215
Cases	United_Arab_Emirates	45,303	57,910	6.8	12,607	27.8	31	25
Cases	Philippines	30,682	41,752	2.6	11,070	36.1	12	259
Cases	Kuwait	40,291	46,889	3.4	6,598	16.4	31	233
Deaths	Peru	8,223	14,544	8.8	6,321	76.9	24	144
Cases	US_Tennessee_Davidson	7,716	13,730	5.3	6,014	77.9	8	423
Cases	Cameroon	12,041	17,830	9.6	5,789	48.1	14	480
Deaths	Russia	8,196	13,573	6.6	5,377	65.6	20	151
Cases	El_Salvador	4,808	9,177	9.2	4,369	90.9	8	492
Cases	Dominican_Republic	27,370	31,447	6.0	4,077	14.9	14	637
Cases	US_Washington_Yakima	6,326	10,266	3.4	3,940	62.3	6	167
Cases	Sudan	8,698	12,425	2.8	3,727	42.8	20	174
Deaths	Bangladesh	1,502	4,870	8.8	3,368	224.2	7	212
Cases	Moldova	14,363	17,669	8.5	3,306	23.0	10	508
Cases	US_Texas_El_Paso	4,553	7,645	7.6	3,092	67.9	12	285
Cases	US_Maryland_Baltimore	7,585	10,177	8.9	2,592	34.2	20	0
Cases	US_Maryland_Anne_Arundel	4,916	7,175	0.1	2,259	46.0	6	1
Cases	US_Nebraska_Douglas	6,386	8,611	0.0	2,225	34.8	13	0
Cases	US_Ohio_Franklin	7,915	9,941	3.3	2,026	25.6	18	97
Cases	US_California_Orange	10,595	12,609	9.8	2,014	19.0	16	301
Cases	Ukraine	38,056	39,656	9.6	1,600	4.2	19	754
Cases	Haiti	5,211	6,480	3.2	1,269	24.4	8	38
Deaths	Indonesia	2,500	3,449	7.1	949	38.0	9	16
Cases	US_Georgia_Gwinnett	6,407	7,219	8.9	812	12.7	16	169
Cases	US_California_San_Diego	11,096	11,875	7.4	779	7.0	23	131
Cases	US_Ohio_Cuyahoga	5,734	6,450	7.6	716	12.5	8	184
Deaths	Argentina	1,043	1,581	9.7	538	51.6	9	59
Cases	US_Georgia_Cobb	3,969	4,488	6.2	519	13.1	28	0
Deaths	Ukraine	1,022	1,539	4.3	517	50.6	9	31
Cases	US_Puerto_Rico	6,564	7,056	7.2	492	7.5	12	152
Cases	US_Pennsylvania_Chester	3,513	3,975	10.0	462	13.2	34	19
Deaths	US_California_Los_Angeles	3,137	3,506	2.7	369	11.8	31	25
Cases	US_Minnesota_Ramsey	4,352	4,675	7.2	323	7.4	23	34
Deaths	Nigeria	525	840	6.2	315	60.0	7	29
Cases	US_Wisconsin_Milwaukee	10,355	10,668	5.5	313	3.0	26	89
Deaths	Armenia	360	666	6.7	306	85.0	9	19
Deaths	US_Florida_Palm_Beach	468	747	7.0	279	59.6	10	14
Deaths	US_Arizona_Maricopa	634	776	8.4	142	22.4	29	9
Deaths	US_Texas_Dallas	317	434	3.0	117	36.9	32	0
Deaths	US_Massachusetts_Bristol	546	663	1.4	117	21.4	26	0
Deaths	US_Ohio_Cuyahoga	339	456	3.3	117	34.5	14	1
Deaths	US_Maryland_Baltimore	455	543	1.4	88	19.3	34	1
Deaths	Sudan	533	615	7.3	82	15.4	10	8
Deaths	US_California_Riverside	424	498	1.4	74	17.5	34	0
Deaths	US_Texas_El_Paso	120	190	7.2	70	58.3	6	5
Deaths	US_Illinois_Kane	252	319	8.1	67	26.6	21	0
Deaths	US_Texas_Tarrant	208	274	2.0	66	31.7	18	0
Deaths	Kuwait	330	396	3.2	66	20.0	18	1
Deaths	US_California_San_Diego	338	397	5.9	59	17.5	36	0
Deaths	Bulgaria	207	265	9.8	58	28.0	16	0
Deaths	US_Ohio_Franklin	358	408	2.8	50	14.0	17	3
Deaths	US_Georgia_DeKalb	165	205	8.5	40	24.2	32	1
Deaths	US_Utah_Salt_Lake	102	140	4.0	38	37.3	10	2
Deaths	US_Colorado_Adams	153	186	4.0	33	21.6	25	0
Deaths	US_Illinois_Lake	401	433	6.5	32	8.0	24	0
Deaths	US_New_Jersey_Mercer	524	556	8.3	32	6.1	46	0
Deaths	US_California_Kern	60	84	1.5	24	40.0	22	0
Deaths	US_Nevada_Clark	400	419	6.2	19	4.8	39	0
Deaths	US_Maryland_Anne_Arundel	200	217	1.9	17	8.5	41	0
Deaths	US_Virginia_Loudoun	84	100	3.0	16	19.0	6	1
Deaths	US_Nebraska_Douglas	80	94	6.0	14	17.5	6	1
Deaths	US_Florida_Hillsborough	115	128	9.8	13	11.3	15	3
Deaths	Panama	521	529	9.7	8	1.5	17	10
Deaths	US_Puerto_Rico	149	156	0.4	7	4.7	44	0
Deaths	US_Ohio_Hamilton	187	192	9.6	5	2.7	26	3
Deaths	US_South_Dakota_Minnehaha	54	55	2.1	1	1.9	29	0

Deaths	Diamond_Princess	13	12	0.0	-1	-7.7	22	0
Cases	US_Texas_Harris	23,047	21,967	9.8	-1,080	-4.7	12	727
Deaths	India	14,011	32,783	4.4	18,772	134.0	8	842
Cases	Azerbaijan	13,207	30,088	8.4	16,881	127.8	6	1324
Cases	Panama	26,752	38,757	8.5	12,005	44.9	7	1553
Cases	US_California_Los_Angeles	86,017	97,102	8.8	11,085	12.9	21	1629
Cases	Russia	591,465	703,979	7.9	112,514	19.0	36	2025
Deaths	WholeWorld	635,463	701,602	1.7	66,139	10.4	39	3482
Cases	Egypt	56,809	171,053	5.9	114,244	201.1	9	4947
Cases	Saudi_Arabia	161,005	337,073	5.7	176,068	109.4	6	5268
Cases	Mexico	185,122	754,786	2.6	569,664	307.7	14	5941
Cases	Bangladesh	115,786	267,358	5.8	151,572	130.9	8	9044
Cases	Pakistan	185,034	470,553	6.5	285,519	154.3	7	17969
Cases	US	2,312,302	2,089,628	9.8	-222,674	-9.6	35	21481
Cases	India	440,215	1,363,036	9.8	922,821	209.6	13	35566
Cases	WholeWorld	11,806,469	15,823,018	2.7	4,016,549	34.0	11	244799
Cases	Iraq	32,676	1	0.0	-32,675	-100.0	-	-
Cases	Oman	31,076	1	0.0	-31,075	-100.0	-	-
Cases	Brazil	1,106,470	1	0.0	-1,106,469	-100.0	-	-
Cases	Argentina	44,931	1	0.0	-44,930	-100.0	-	-
Cases	Poland	32,227	1	0.0	-32,226	-100.0	-	-
Cases	Qatar	88,403	1	0.0	-88,402	-100.0	-	-
Cases	Chile	246,963	1	0.0	-246,962	-100.0	-	-
Cases	South_Africa	101,590	1	0.0	-101,589	-100.0	-	-
Cases	Bulgaria	3,984	1	0.0	-3,983	-100.0	-	-
Cases	Colombia	71,367	1	0.0	-71,366	-100.0	-	-
Cases	North_Macedonia	5,196	1	0.0	-5,195	-100.0	-	-
Cases	US_Florida_Broward	11,327	1	0.0	-11,326	-100.0	-	-
Cases	US_Nevada_Clark	10,774	1	0.0	-10,773	-100.0	-	-
Cases	Armenia	20,588	1	0.0	-20,587	-100.0	-	-
Cases	US_California_Alameda	5,007	1	0.0	-5,006	-100.0	-	-
Cases	US_California_Riverside	13,800	1	0.0	-13,799	-100.0	-	-
Cases	Senegal	5,970	1	0.0	-5,969	-100.0	-	-
Cases	US_Texas_Dallas	17,299	1	0.0	-17,298	-100.0	-	-
Cases	Bolivia	25,493	1	0.0	-25,492	-100.0	-	-
Cases	Kazakhstan	18,231	1	0.0	-18,230	-100.0	-	-
Cases	US_Florida_Palm_Beach	10,943	1	0.0	-10,942	-100.0	-	-
Cases	US_Georgia_DeKalb	4,791	1	0.0	-4,790	-100.0	-	-
Cases	US_North_Carolina_Mecklenburg	8,956	1	0.0	-8,955	-100.0	-	-
Cases	US_Arizona_Maricopa	31,650	1	0.0	-31,649	-100.0	-	-
Cases	US_Florida_Hillsborough	5,973	1	0.0	-5,972	-100.0	-	-
Cases	US_Texas_Bexar	6,882	1	0.0	-6,881	-100.0	-	-
Cases	US_Texas_Travis	6,210	1	0.0	-6,209	-100.0	-	-
Cases	Congo_Kinshasa	5,924	1	0.0	-5,923	-100.0	-	-
Cases	Honduras	13,356	1	0.0	-13,355	-100.0	-	-
Cases	US_Texas_Tarrant	8,955	1	0.0	-8,954	-100.0	-	-
Cases	Guatemala	13,769	1	0.0	-13,768	-100.0	-	-
Cases	Nigeria	20,919	1	0.0	-20,918	-100.0	-	-
Cases	US_Arizona_Pima	5,587	1	0.0	-5,586	-100.0	-	-
Cases	US_Tennessee_Shelby	8,064	1	0.0	-8,063	-100.0	-	-
Cases	Kenya	4,797	1	0.0	-4,796	-100.0	-	-
Cases	US_California_San_Bernardino	9,361	1	0.0	-9,360	-100.0	-	-
Cases	US_Ohio_Hamilton	4,020	1	0.0	-4,019	-100.0	-	-
Cases	US_California_Kern	3,965	1	0.0	-3,964	-100.0	-	-
Cases	US_Pennsylvania_Lancaster	4,029	1	0.0	-4,028	-100.0	-	-
Deaths	Iraq	1,167	1	0.0	-1,166	-99.9	-	-
Deaths	Egypt	2,278	1	0.0	-2,277	-100.0	-	-
Deaths	Pakistan	3,695	1	0.0	-3,694	-100.0	-	-
Deaths	Mexico	22,584	1	0.0	-22,583	-100.0	-	-
Deaths	US_Georgia_Fulton	304	1	0.0	-303	-99.7	-	-
Deaths	Colombia	2,426	1	0.0	-2,425	-100.0	-	-
Deaths	Chile	4,502	1	0.0	-4,501	-100.0	-	-
Deaths	North_Macedonia	247	1	0.0	-246	-99.6	-	-
Deaths	Saudi_Arabia	1,307	1	0.0	-1,306	-99.9	-	-
Deaths	Honduras	395	1	0.0	-394	-99.7	-	-
Deaths	US_California_Orange	269	1	0.0	-268	-99.6	-	-
Deaths	South_Africa	1,991	1	0.0	-1,990	-99.9	-	-
Deaths	Afghanistan	598	1	0.0	-597	-99.8	-	-
Deaths	Belarus	351	1	0.0	-350	-99.7	-	-
Deaths	Bolivia	820	1	0.0	-819	-99.9	-	-
Deaths	US_Washington_Yakima	138	1	0.0	-137	-99.3	-	-
Deaths	Azerbaijan	161	1	0.0	-160	-99.4	-	-
Deaths	Kazakhstan	127	1	0.0	-126	-99.2	-	-
Deaths	US_Minnesota_Ramsey	211	1	0.0	-210	-99.5	-	-
Deaths	Guatemala	547	1	0.0	-546	-99.8	-	-
Deaths	Oman	137	1	0.0	-136	-99.3	-	-
Deaths	Qatar	99	1	0.0	-98	-99.0	-	-
Deaths	Haiti	88	1	0.0	-87	-98.9	-	-
Deaths	Senegal	86	1	0.0	-85	-98.8	-	-